Chapter 6

Forward SHM for Delamination

6.1 Introduction

Composite is changing the world of structural construction due to its various technological advantages. However, these new materials also have some problems such as fiber breakage, matrix cracking, and delamination. Matrix cracks and fiber breakages play an important role in laminates under tensile load. But, the primary concern with polymer composites is the delamination failure, which is debonding of adjacent plies, since the through-thickness properties of composite laminates are typically matrix dominated and therefore, much weaker than the fiber dominated in-plane properties. In industry, one of the commonly encountered types of defect or damage in laminated composite structures is delamination. Delamination often occur at stress free edges due to the mismatch of properties at ply interfaces and it can also be generated by external forces such as out of plane loading or impact during the service life. While such impact can cause a number of delaminations, a small surface indentation is the only external indication since the delaminations are cracks in the interior of the laminate. Thus, this type of damage is often called barely visible impact damage, which is not readily identified by visual inspection. This problem is caused from the fact that transverse tensile and interlaminar shear strength of composite laminates are quite low in contrast to their in-plane properties. Inter layer debonding or delamination is a prevalent form of damage phenomenon in laminated composites. It may be formed due to a wide variety of foreign object impact damage, poor fabrication process, and fatigue from environmental cycling. Delaminations cause a reduction in the stiffness of the structure thus affecting its vibration characteristics. They also substantially reduce the buckling load capacity, which, in turn, influences the stability characteristics of the structure. Hence, delamination is the critical parameter for laminates under compression and one of the most common failure modes in composite laminates. Kim et al. [183]

had studied the effects of delaminations in composite plate. Delamination of composite laminate had been studied in structural health monitoring context by many researchers [72, 234, 247, 285, 332, 348, 350, 352, 370, 418].

In this chapter, numerical simulation are carried out for a delaminated composite laminate with or without magnetostrictive patches as sensors and actuators using anhysteretic, coupled, linear properties of magnetostrictive materials. Effect of delamination in cantilever tip velocity and sensor open circuit voltages are studied. Single and multiple delaminations are studied with tip vertical impact load and biased sinusoidal current in actuator coil. The presence of delamination, changes the stress response of the structure. This in turn changes the magnetic flux density of the magnetostrictive sensor. The changes in the flux density are sensed through a sensing coil as open circuit voltage. Measurement of open circuit voltage before and after the damage (delamination) occurrence provides a diagnostic measure to indicate the presence of the damage.

This chapter is organized as follows. First the modelling of delamination considering beam and 2D plane stress formulation is studied and compared for both static tip deflection and natural frequencies of a cantilever beam. Then the tip deflection histories, due to tip vertical load on a delaminated cantilever beam are studied for different size and location of delamination. Next, due to the same tip load, sensor open circuit voltages are studied for different delamination configurations. To study the effect of location of sensor in response histories, one delaminated portal frame is studied with different locations of sensors with a fixed location of delamination and actuator. Although beam assumption reduces the computational cost, it introduces the errors from its inherent assumption. The relative importance between the errors due to different beam assumptions and the sensitivity of the delamination for both thick and thin portal frame is studied. Finally, the effect of different delamination configuration on tip deflection and sensor response due to actuation in two different frequencies are studied. The chapter is then concluded with a brief summary.

6.2 Delamination Modelling in Composite Laminate

Many stiffness and modulus degradation models have been proposed in the literature for finite element modelling of damage, which is not suitable for modelling of delamination in composite structure. Literature for modelling of delamination is discussed in the introductory chapter of Section-1.2.5.2.

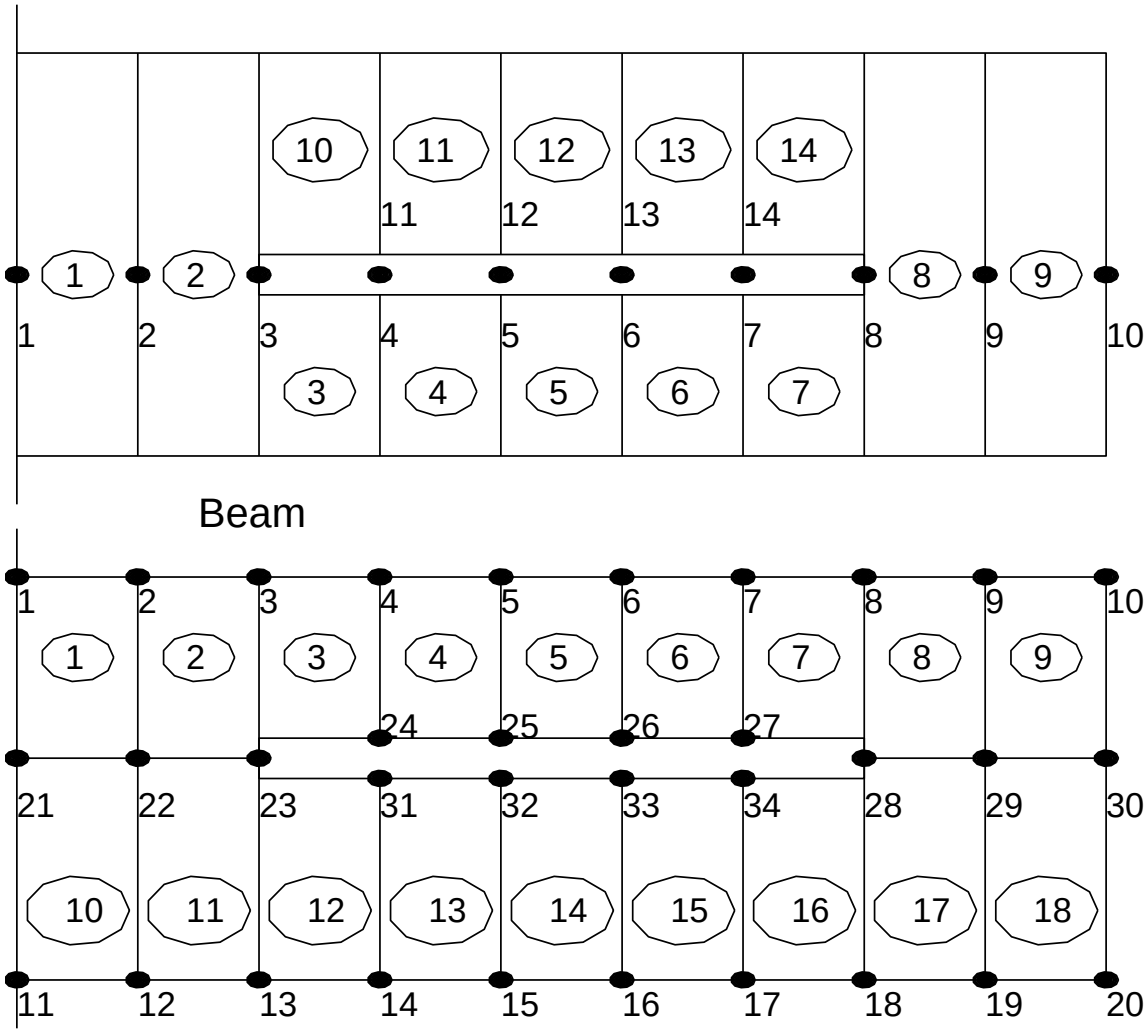

Figure 6.1: Modelling of Delamination in Finite Element Formulation.

In this chapter, modelling of delamination in finite element is done through keeping two nodes in same place, one for the elements above the delamination and other for below. Modelling of delamination for beam and 2D plane stress/ plane strain assumption is shown in Figure-6.1. For beam formulation, elements 1 and 2 are at the left part, and, elements 8 and 9 are at the right part of the delaminated zone. All other elements are in the delaminated zone, either at the above or below the delamination. Zone below the delamination is modelled with elements 3 to 7 and above by elements 10 to 14. Delamination is modelled through proper nodal connectivity of these elements. That is,

for healthy zone, element 1 is connected with nodes 1 and 2; and element 9 is connected with nodes 9 and 10. All these nodes are in the mid plane of the corresponding beam elements. For element below the delamination, like, element 3 is connected with nodes 3 and 4, where, the nodes 3 and 4 are not in the mid plane of this element. This may create high bending-stretching coupling. Similarly, for element above the delamination, like, element 10 is connected through nodes 3 and 11, where nodes 3 and 11 are not in the mid plane of this element. As mention earlier, nodes 4 and 11 are in the same place and not connected with any direct element. These are termed as duplicate nodes. Similarly, (5 and 12), (6 and 13) and (7 and 14) nodes are the duplicate nodes. In the delaminated zone, lower part of the elements connects with nodes 4, 5, 6, and 7 and upper parts of the elements connect nodes 11, 12, 13, and 14. If these nodes are merged with their corresponding duplicate nodes, the beam will be healthy. In addition, with these duplicate nodes, different kind of contact or gap elements can be used in finite element analysis.

In the literature, for 2D plane stress/strain assumption, delamination is modelled using such duplicate nodes. Nodes 24, 25, 26 and 27 are connected with the elements for above the delamination, and their corresponding duplicate nodes are 31, 32, 33 and 34, which are connected with elements below of the delamination respectively. Elements below the delamination, like element 12 is connected with nodes 13, 14, 31 and 23, and elements above the delamination, like element 3 is connected with nodes 23, 24, 4 and 3. These two elements have duplicate nodes 24 and 31. Similarly, (25, 32), (26, 33) and (27, 34) are duplicate nodes for other elements exist below and above the delamination. Multiple delaminations can also be modelled in similar manner for both beam and 2D assumption. Static and free vibration study for a unidirectional laminated cantilever beam is performed to demonstrate the efficiency of the present delamination modelling strategy.

Figure-6.2(a) shows the percentage increase of static tip deflection due to mid layer delamination near the support of a cantilever beam. When the delamination is 10 % of the length of the cantilever, beam assumption shows 0.39% of increase of static tip deflection. But when the 90% of the cantilever is delaminated, the increase of static tip deflection is 55.16%. Corresponding percentage increase of deflection due to 2D model is 0.3% to 0.4% lower than the beam formulation. Hence, it clearly indicates, present delamination model of beam can be used for static analysis with in 0.5% accuracy.

Figure-6.2(b) shows the decrease of first 15 natural frequencies due to mid layer

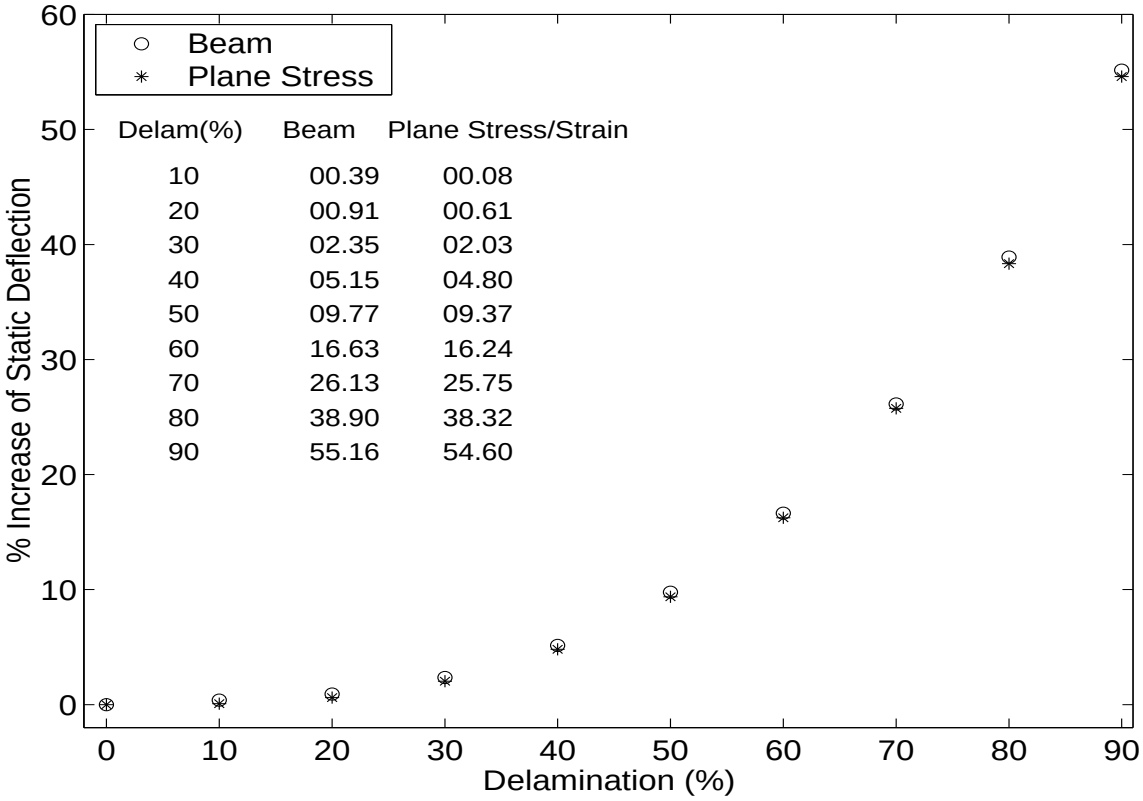

(a) Static Tip Deflection

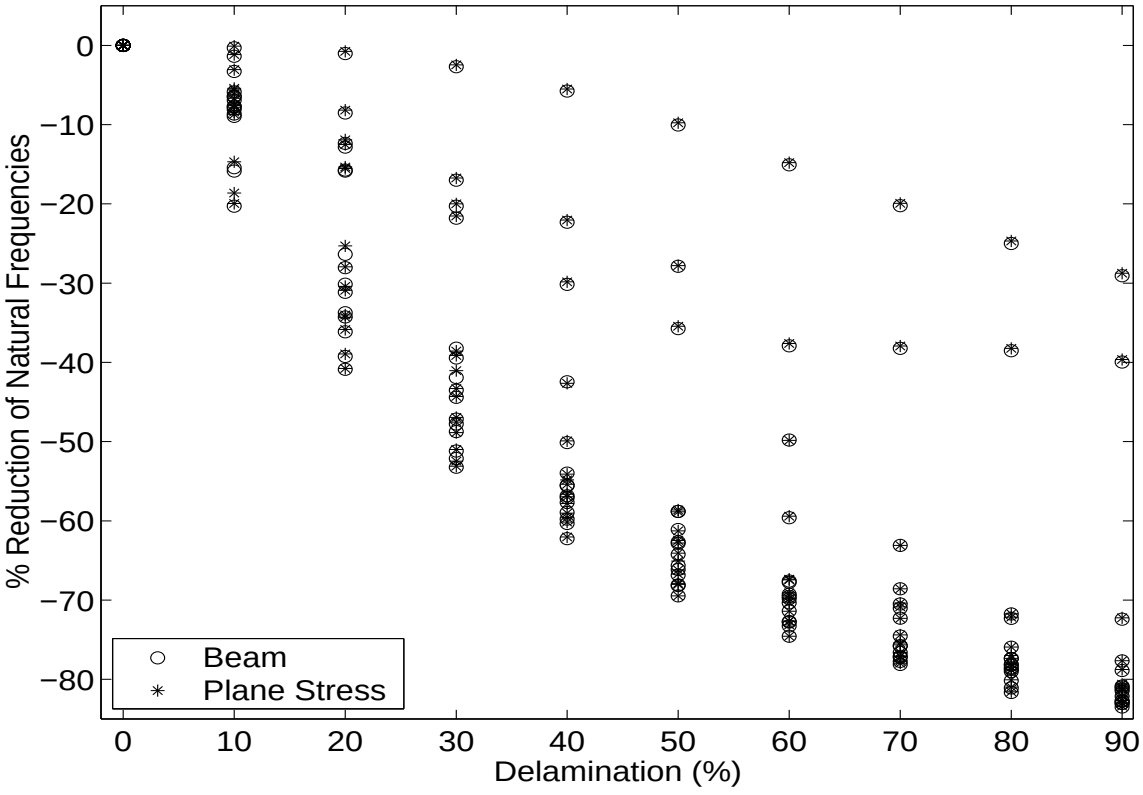

(b) Free Vibration

Figure 6.2: Comparison between Beam and 2D Modelling of Delamination

delamination near the support of a cantilever beam. Both the models (beam and 2D) show more or less similar results. When the delamination is 10 % of the length of the cantilever, 15^{th} natural frequency reduces 20% than the corresponding frequency of the healthy beam. Similarly, for 90% delamination, first natural frequency reduces 29%, second natural frequency reduces 40% and third natural frequency reduces 72%. This study shows that the results of static and dynamic simulations for beam and 2D-plane stress/strain models give results that match very well. In the next section, with this modelling technique of delamination, structural responses of a delaminated cantilever beam are studied.

6.3 Numerical Example

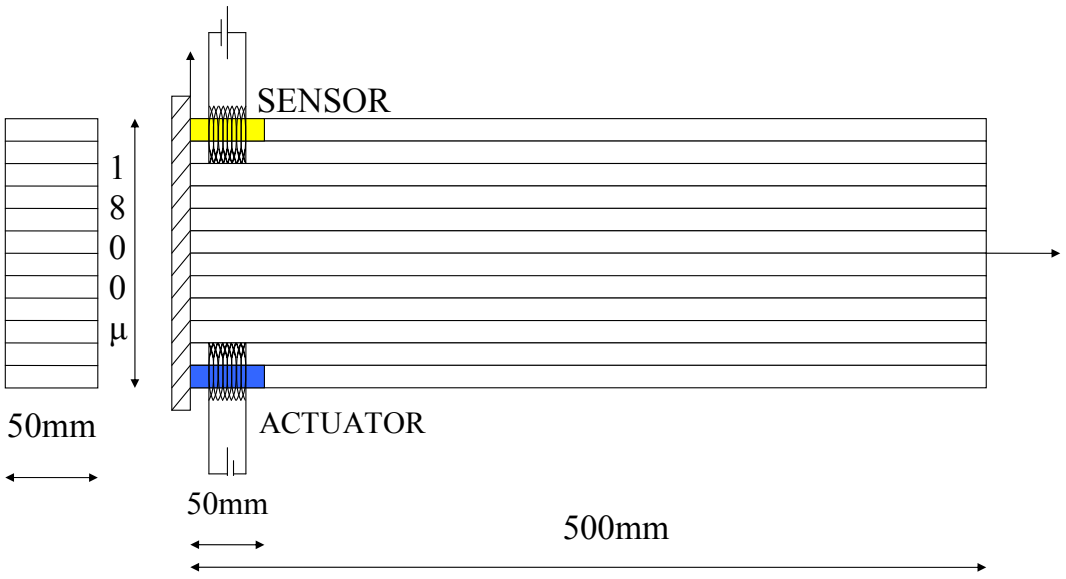

Figure 6.3: Composite Beam with Sensor and Actuator

In this section, a cantilever beam is considered to explore the use of magnetostrictive sensors and actuators for a time domain health monitoring application. Numerical simulation is carried out by assuming a unidirectional laminated composite beam of total thickness 1.8mm as shown in Figure-6.3. Length and width of the beam is 500mm and 50mm respectively. The beam is made of 12 layers with thickness of each layer being 150 μ-m. Position of sensor and actuator are fixed at top and bottom layer of the

beam respectively. Both the sensor and actuator are placed near the support of the cantilever. Size of the actuator and sensor are 50mmX50mm with 150 μ-m thickness. Elastic modulus of composite is 181 GPa and 10.3 GPa in parallel (E_1) and perpendicular (E_2) direction of fiber. Poisson's ratio (ν), density (ρ) and shear modulus (G_{12}) of composite is assumed 0.0, 1.6 gm/c.c. and 28 GPa respectively. Elastic modulus (E_m), Poisson's ratio (ν_m), shear modulus (G_m) and density (ρ_m) of magnetostrictive material is 30 GPa, 0.0, 23 GPa and 9.25 gm/c.c. respectively. Magneto-mechanical coupling coefficient is 15 nano-m/amp for sensing and actuation properties of magnetostrictive material. Relative permeability of magnetostrictive material has been considered as 10. Number of coil turn in sensor and actuator are 20000 turn/m (1000 turn).

Figure-6.4 to Figure-6.16 are the response histories for different delaminated and healthy cantilever beam. Continuous lines are the response for healthy and dotted lines are for delaminated beam. Cantilever beam showing delamination with position and size is plotted in the inset of the corresponding figures.

6.3.1 Tip Response Due to Tip Load

Figure-6.4 to Figure-6.10 are the vertical velocity histories due to vertical load in the tip of the cantilever. Load history and its frequency content are shown in the Figure-5.13(a). For healthy beam, waves reflected from support and arrived after 1 mili-sec. For delaminated beams, these waves will be scattered from delamination tip and reflected back from the delaminated zone. Hence from the arrival time of the reflected wave, location of delamination zone can be identified. Similarly, the deviation of the response from healthy beam response gives some information about the size of the delamination. If the deviation is more delamination size is more.

6.3.1.1 Varying Location

Figure-6.4 shows the cantilever tip velocity for 100mm delamination at mid layer and for different distance from support (0, 80, 160, 240, 320, and 400mm). As mentioned earlier the reflected waves arrived much earlier for delamination near the tip than for delamination near the support. For delamination near the support, difference of the responses starts from 1 milli-sec. But when the delamination is at the free end (400mm from support) of the cantilever, response difference start from 0.35 milli-sec.

Figure-6.5 shows the cantilever tip velocity for 20mm delamination at mid layer and for different distance from support (0, 80, 160, 240, 320, and 400mm). As pointed out in

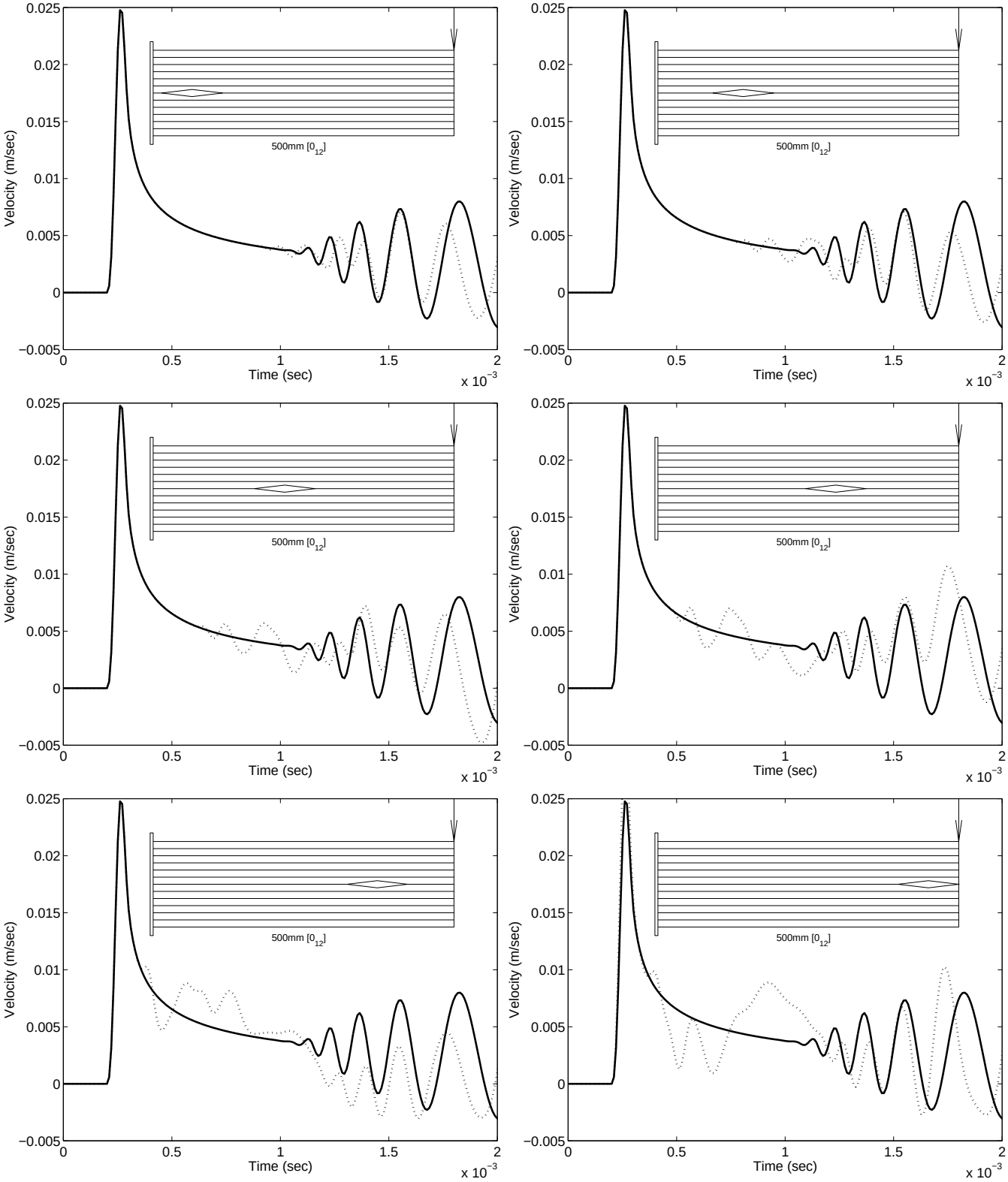

Figure 6.4: 100mm Delamination at Mid Layer and Different Distance from Support.

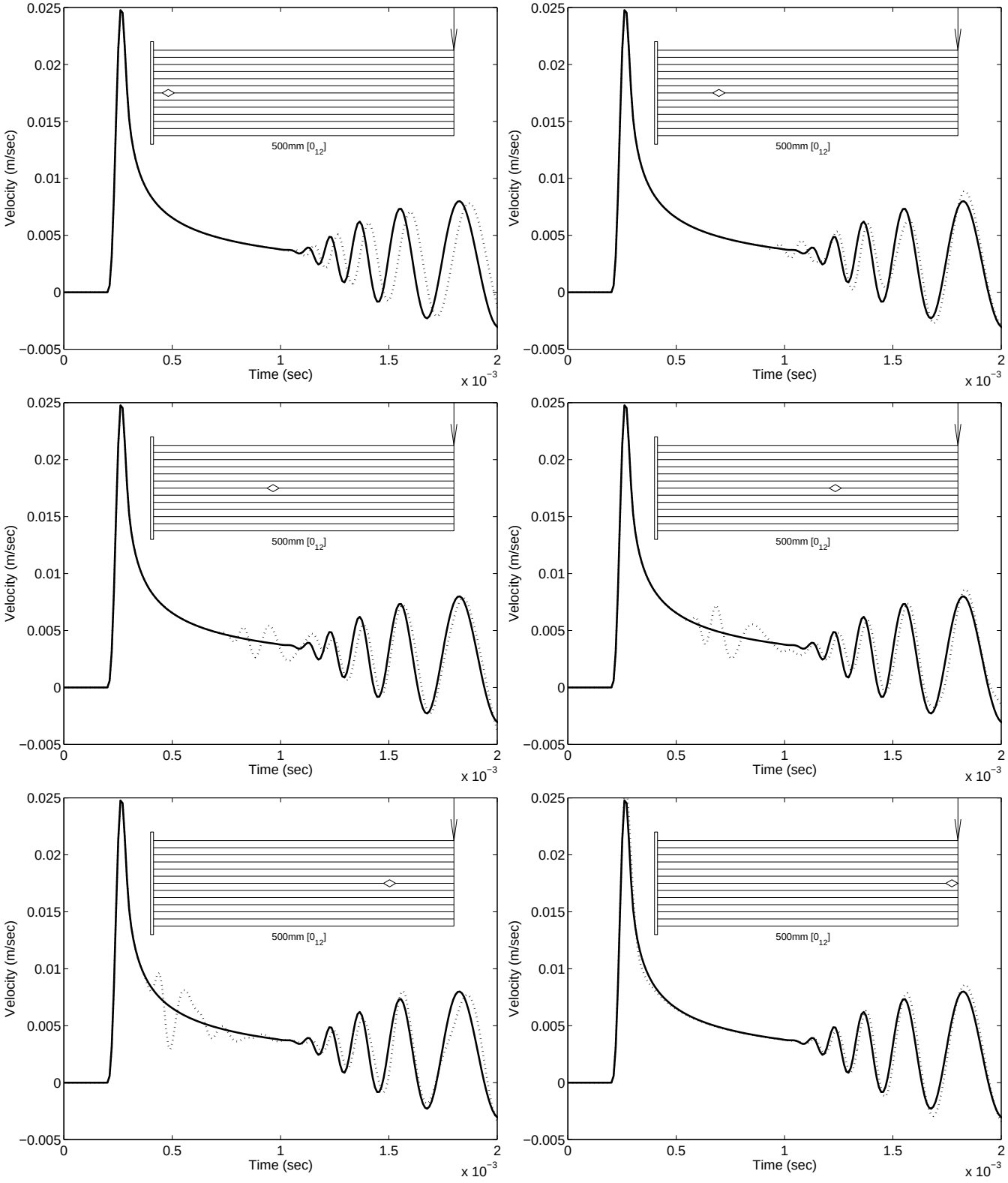

Figure 6.5: 20mm Delamination at Mid Layer and Different Distance from Support.

the earlier Figure, the reflected waves arrived much earlier for delamination near the tip than for delamination near the support. Comparing Figure-6.4 and Figure-6.5 it is clear that the deviation of response for delaminated beam from response of healthy beam is more if the size of the delamination is more.

6.3.1.2 Varying Size

Figure-6.6 shows the responses for different sizes (10, 20, 30, 50, 75, 100mm) of delamination at mid span and at the middle layer of the beam. For 10mm delamination, the deviation is negligible, where as for 100mm delamination, deviation is quite large. In addition, disturbance in the response for reflection from support is less for the smaller delamination. The initial deviation of the response histories are always appear in the same time of the response, which clearly indicate that the location of the delamination is same for all the cases.

Depth wise location of the delamination will also affect the baseline response. Figure-6.7 shows the responses of a delamination of varying size and located at top layer of the beam. Although the reflection arrival time is similar to the response of mid layer delamination, the magnitude of the deviation from the healthy beam response is smaller. However, within the layer, if the size of delamination is increased, the amplitude of the deviation of response form healthy response is also increased. Hence, if delamination layer is identified, size of the delamination can be identified from the magnitude of the deviation of the responses. Moreover, the initial appearance of the disturbance in time history clearly indicates that the location of the delamination is same for all the cases.

6.3.1.3 Symmetric Delaminations

Figure-6.8 and Figure-6.9 show the response histories for different size (10, 20, 30, 50, 75, 100mm) of symmetric delaminations at the mid span of the beam. Figure-6.8 shows the response history for two delaminations at mid span of the beam, one at top layer and other in bottom layer. Initial reflections from delamination in response history for this symmetric delamination is increased up to 30mm delamination size and again reduced for longer delaminations. The disturbance of reflection from support is increased for increased size of delamination.

Figure-6.9 shows the response histories for the symmetric delamination, which makes three equal depth beams at delaminated zone. Here, the effect of delamination in response histories are more, even for 10mm delamination sizes. Moreover, the distur-

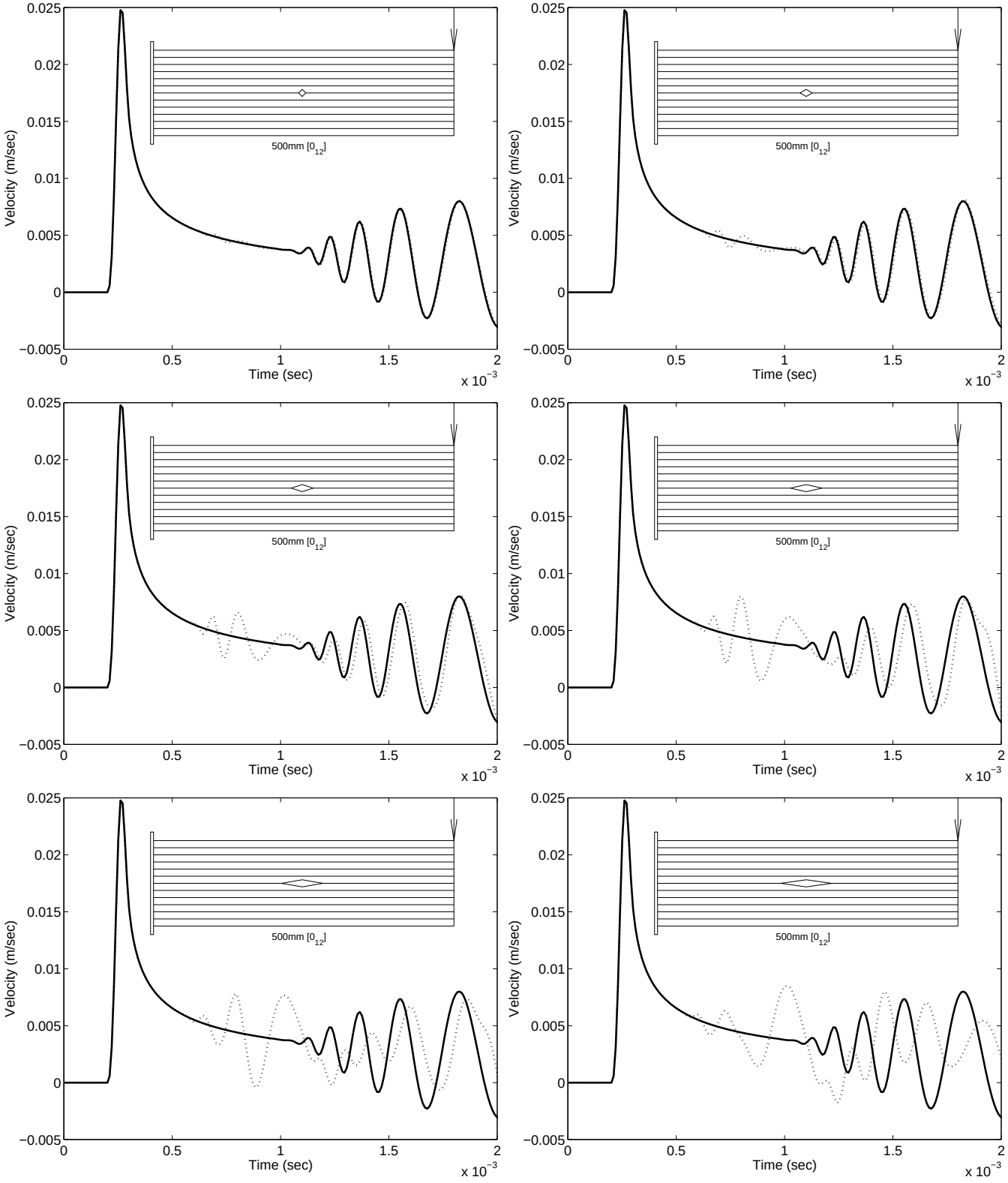

Figure 6.6: Delamination at Mid span of Mid Layer with Different sizes.

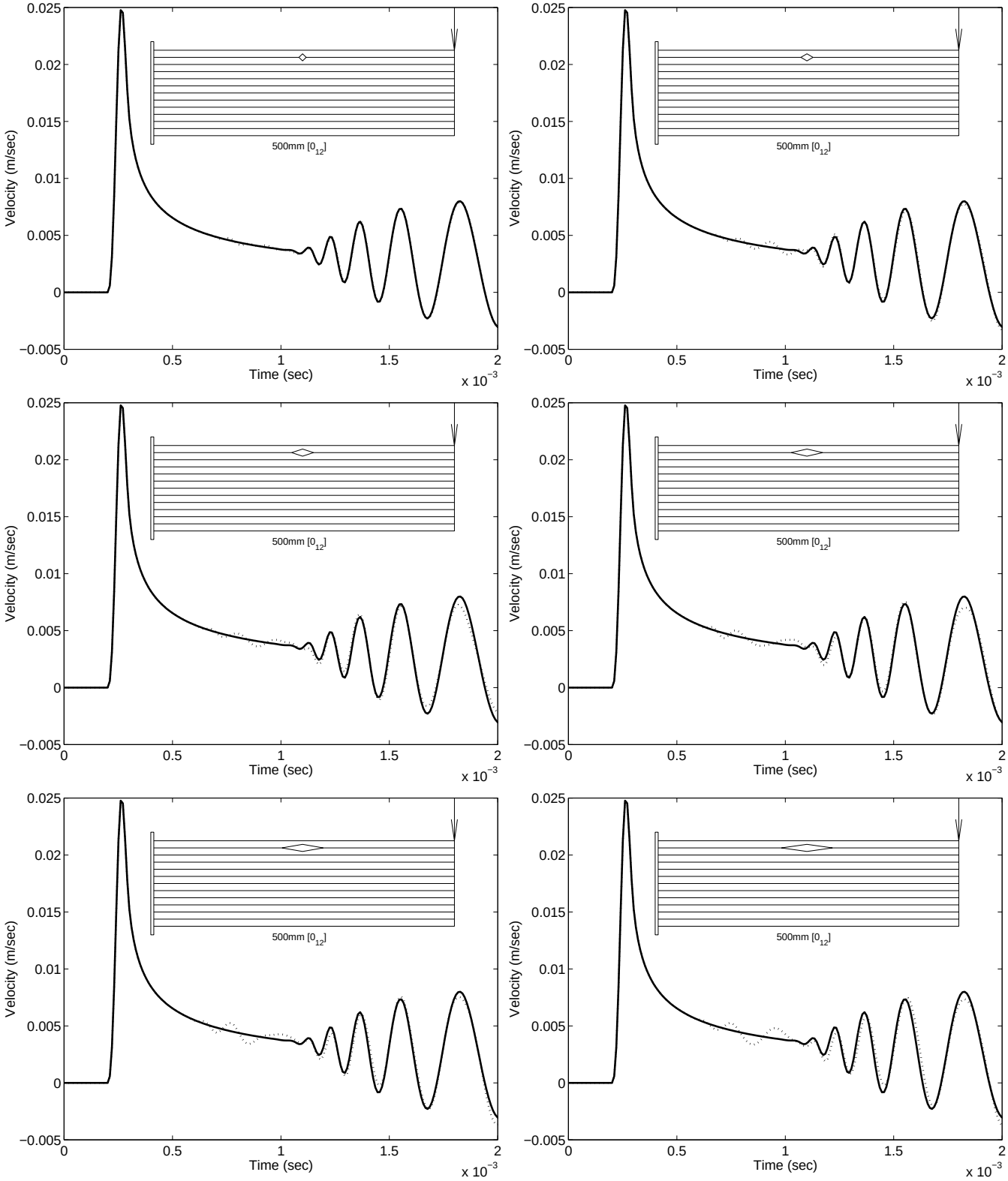

Figure 6.7: Delamination at Mid span of Top Layer with Different sizes.

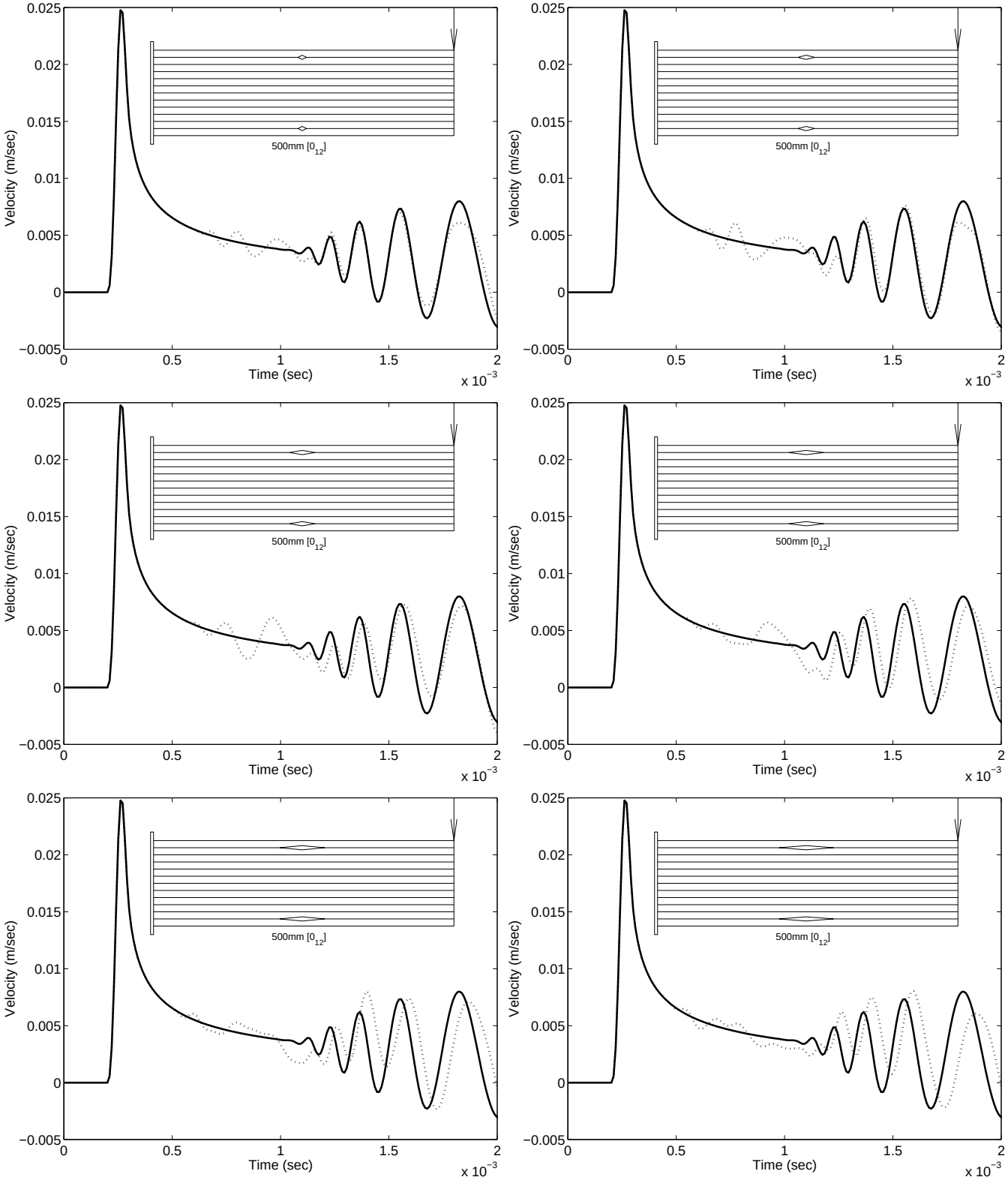

Figure 6.8: Symmetric Delaminations at Top and Bottom Layers.

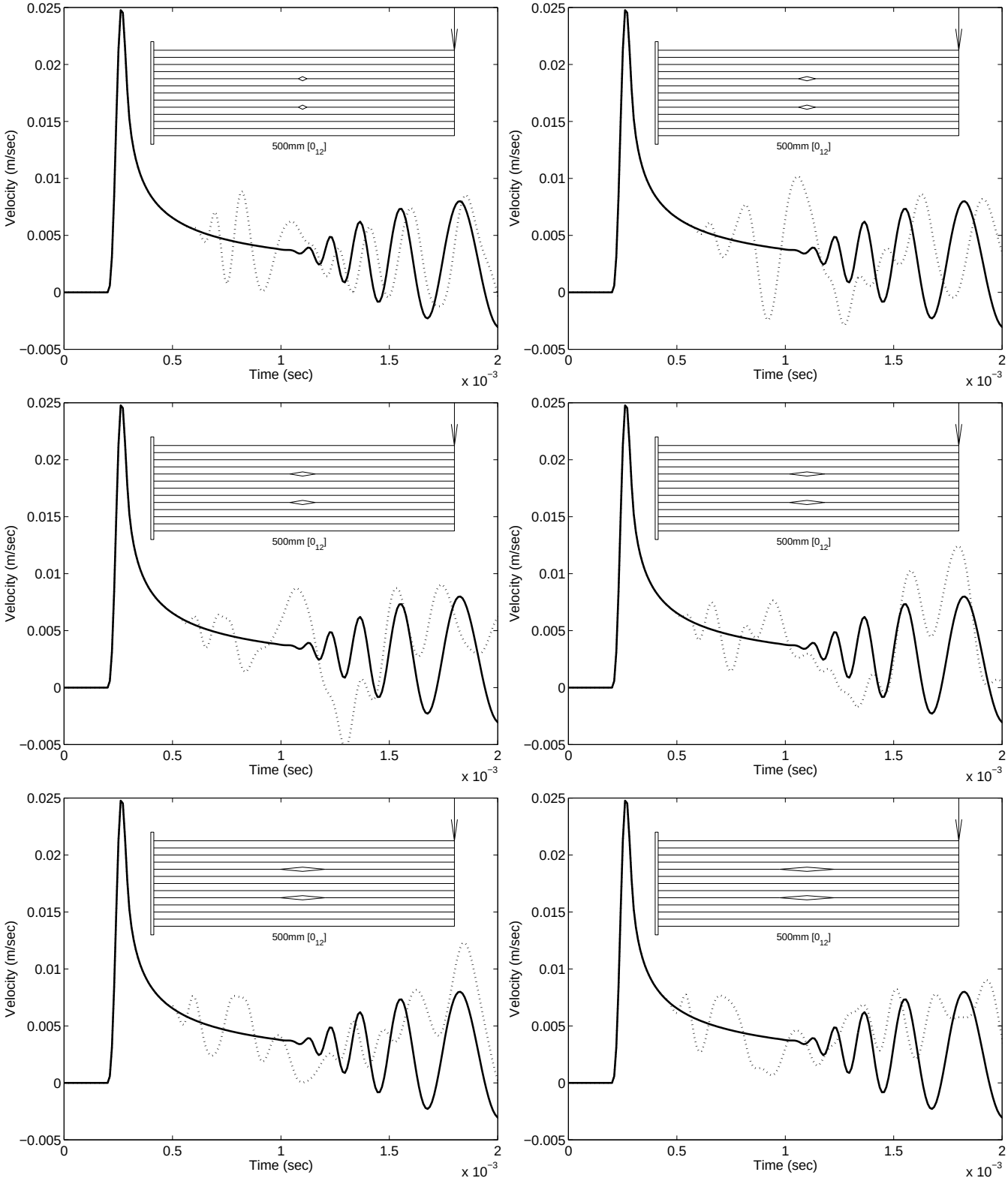

Figure 6.9: Symmetric Delaminations at ± 0.3mm Layers.

bance of support reflection is also large compared to symmetric delamination at top and bottom layers. Hence, for symmetric delamination, if the sub-laminates are equally thick, deviation in the response histories will be more relative to the delaminations at top and bottom layer. Initial reflection from delamination in response history is increased up to 30mm delamination size and again reduced for longer delaminations. This 30mm size of delamination may have some specific relation to the symmetric delamination. Location of initial disturbances indicates that the delamination location along the span of the beam is same for all the cases.

6.3.1.4 Multiple Delaminations

Multiple delaminations occur due to impact loading in the composite laminates and the sizes of the delaminations are increased towards the depth of the laminates. Due to this delamination profiles, identification of delamination using vibration properties of the beam is easier than other conventional methods. Figure-6.10 shows response histories for the multiple delaminations of size increasing towards the depth of the beam with three to six layers of delaminations. Initial appearances of deviation of response histories are same for all the cases, which can be used to identify the span location of the delamination. But the magnitude of the deviation is completely different for different number of delaminated layers. Every response histories have their unique pattern. Like, initial deviation of response histories for three layer delaminations is more than four layer delaminations. Hence, there is no direct relation between the delaminated layer numbers with the deviation of the responses. More importantly, phase shift for three layer delamination is less and it is increased gradually for more number of layers, which can be used as a condition to identify the number of delaminated layer.

6.3.2 Sensor Response for a Tip Load

Figure-6.11 to Figure-6.16 give the open circuit voltage histories due to vertical load applied at the tip of the cantilever. Load history is shown in Figure-5.13(a) with its frequency content. Sensor of size 50mmX50mmX150 μ-m is placed near the support of top layer. Cantilever beam showing delamination and sensor with position and size is plotted in the inset of the corresponding figures. Although the tip load is applied after 200 μ-sec, the stress waves and hence open circuit voltages appear only after 500 μ-sec, which is due to required time to travel the stress waves from impacted point to sensor location.

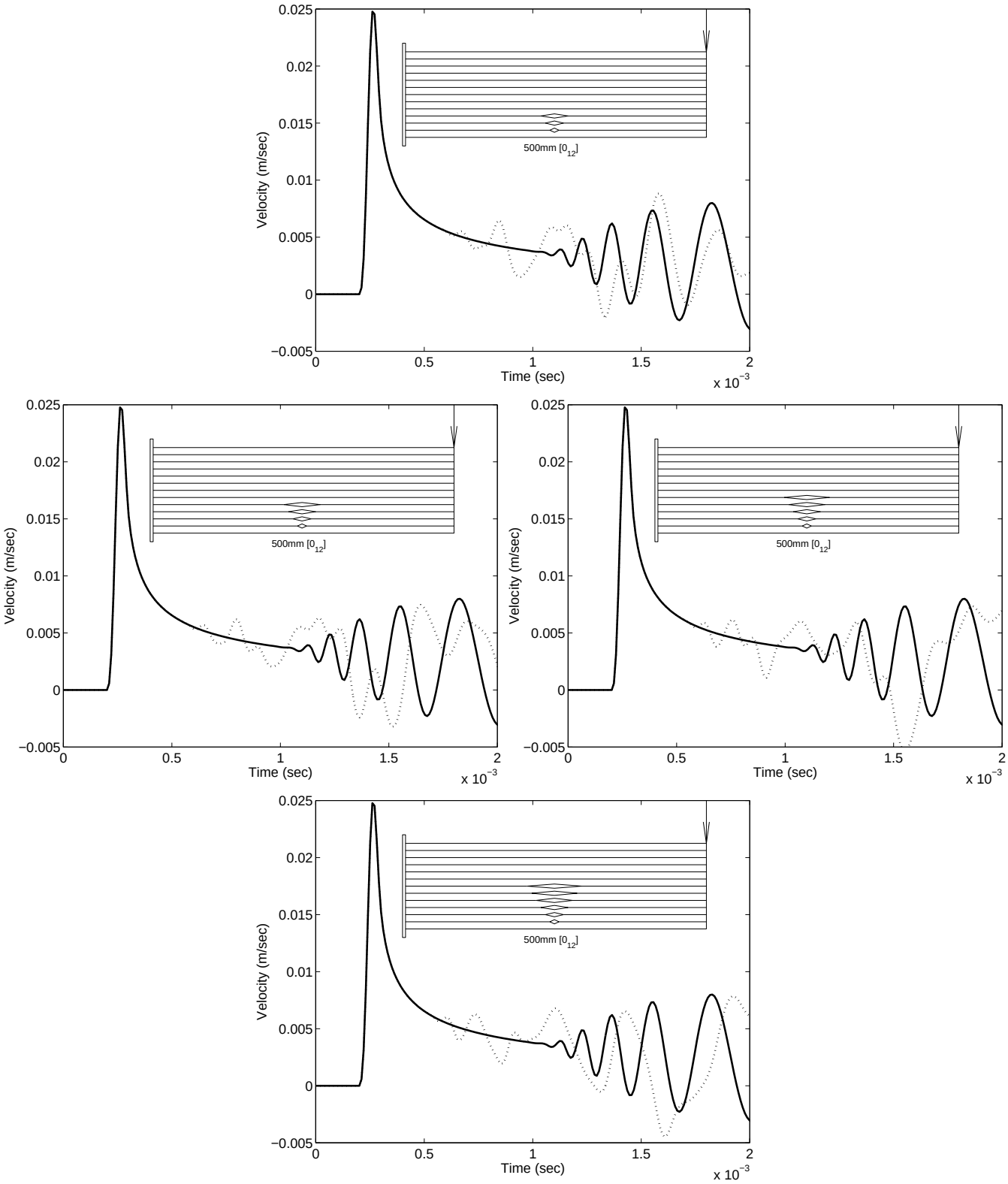

Figure 6.10: Multiple Delaminations Increasing towards the Depth.

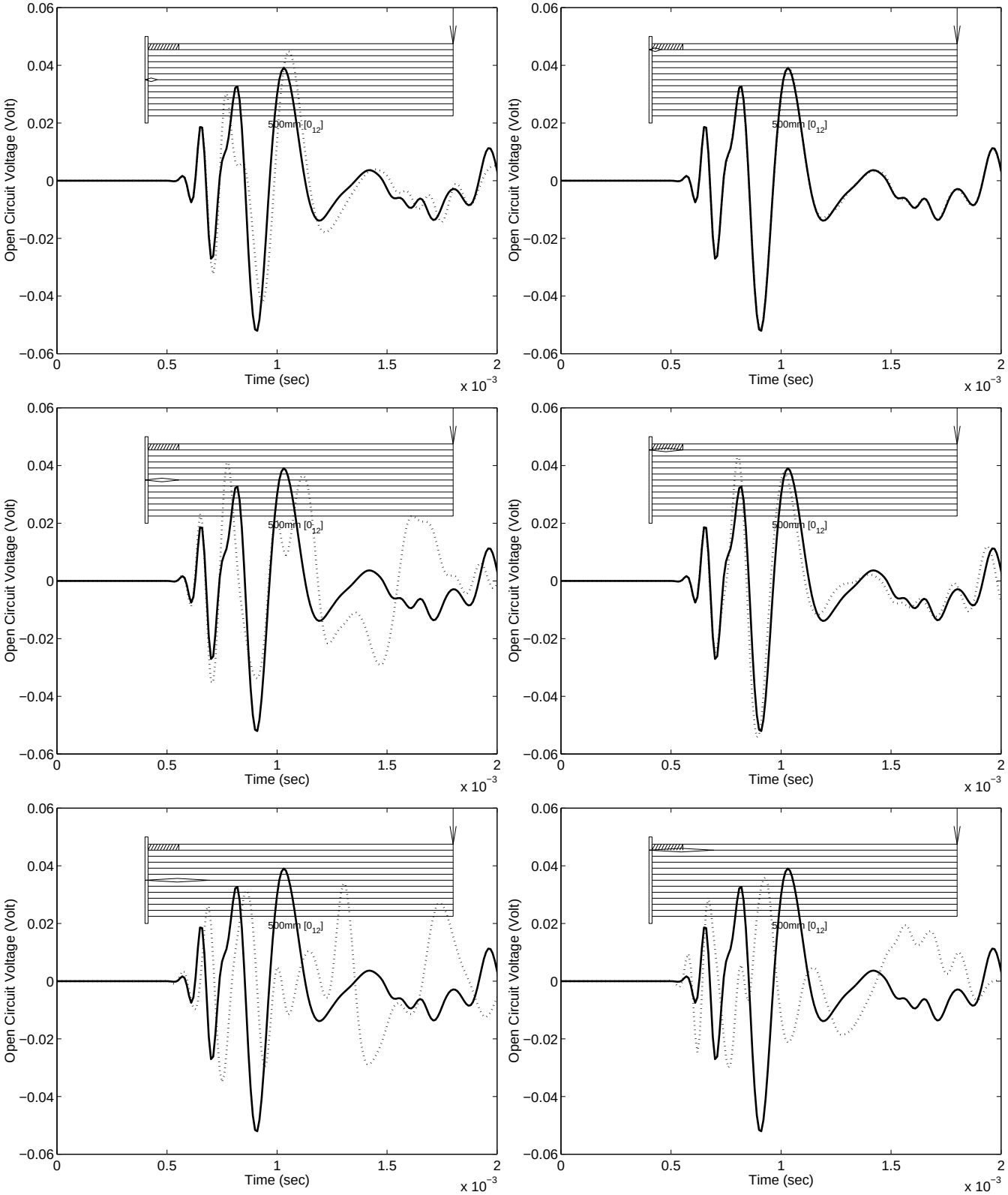

Figure 6.11: 20, 50 and 100mm Delamination at mid and top Layer near Support.

6.3.2.1 Varying Size and Layer

Figure-6.11 shows the open circuit voltage in the sensor coil due to cantilever tip impact load with 20, 50 and 100mm single delamination at top layer and mid layer. The effect of delamination in open circuit voltages for 20mm delamination below the sensor is not recognizable. The same size delamination at mid layer however is showing considerable response deviation with little phase shift. Similarly, delamination at top layer has less effect than delamination at mid layer for 50mm size, and this is more after 1 milli-sec of response. Contrary to the previous case, the initial phase shift of the open circuit voltages from healthy beam are more for 100mm delamination below sensor than same delamination at middle layer. Hence, with phase shift and magnitude of the deviation of the sensor response, size and layer of the delamination can be identified using some mapping technique.

6.3.2.2 Varying Location

Delamination near the sensor was studied earlier. In this subsection, the effect of delamination away from the sensor is studied for delamination at top, bottom and mid layer of the beam. Figure-6.12 shows the open circuit voltages for 100mm top layer delamination for different distance (40, 50, 60, 70, 80, and 90mm) from support. When the distance between delamination and sensor is increased, the changes in the sensor response are decreased. For delamination located at 90mm from support, the effect of delamination in sensor response is negligible. Similar to amplitude of response, phase shifts are found to be more when the delaminations are near the sensor. Hence, the phase shift and the amplitude of response history can be used for identification of the location of delamination.

Figure-6.13 shows the open circuit voltages for 100mm mid layer delamination for different distance (40, 50, 60, 70, 80, and 90mm) from support. Unlike top layer, at mid layer, for delamination located 90mm away from support, the effect of delamination in sensor response is also considerable for identification. Location and amplitude of peak response is also varied considerable for different location of delamination. Hence, if the delamination is in the mid layer, identification of the location of delamination from magnitude and phase shift of sensor response is possible even at sufficient distance away from the sensor.

Figure-6.14 shows the open circuit voltages for 100mm bottom layer delamination for different distance (40, 50, 60, 70, 80, and 90mm) from support. Effect of bottom layer

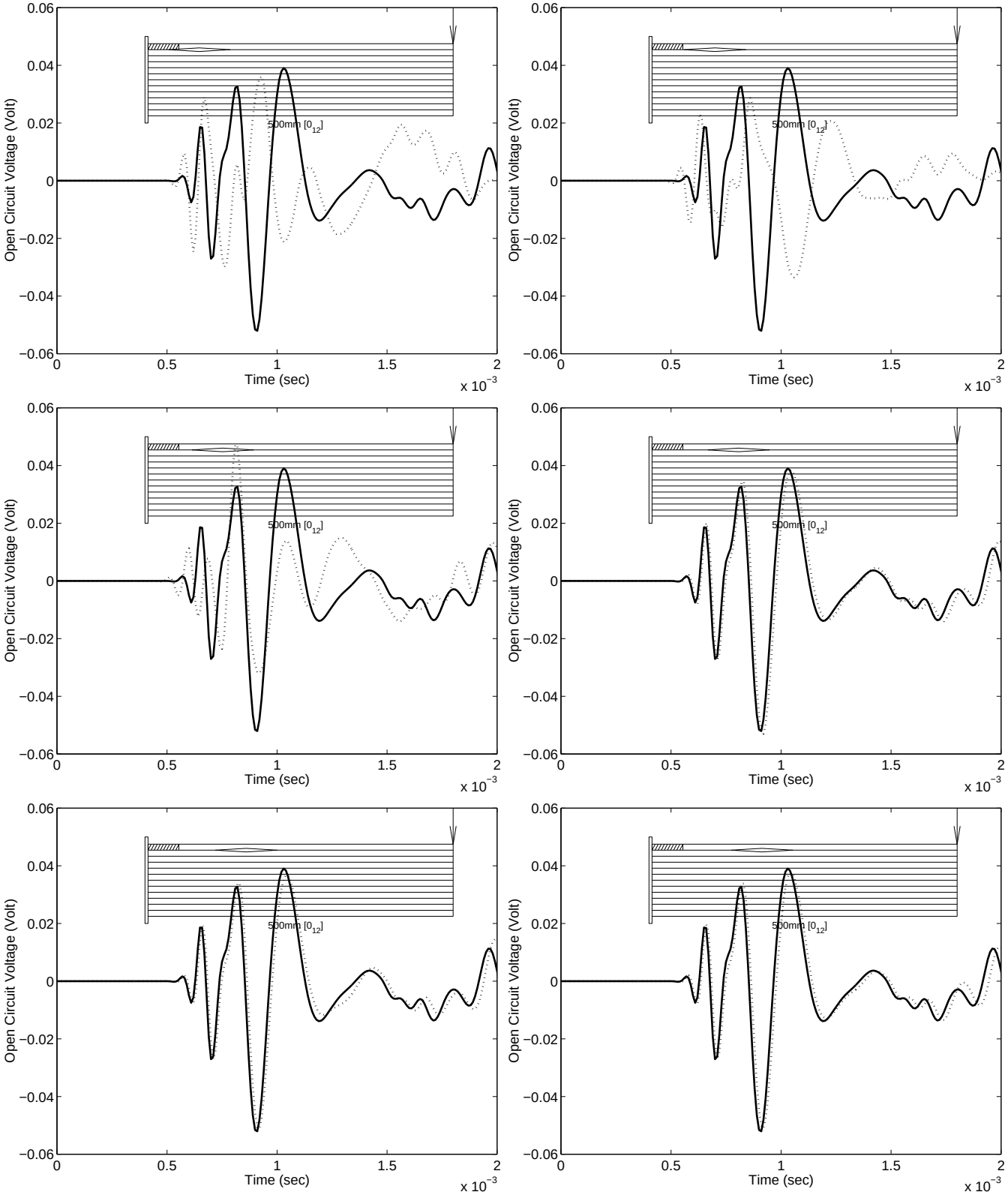

Figure 6.12: 100mm Top Layer Delamination for Different Distance from Support.

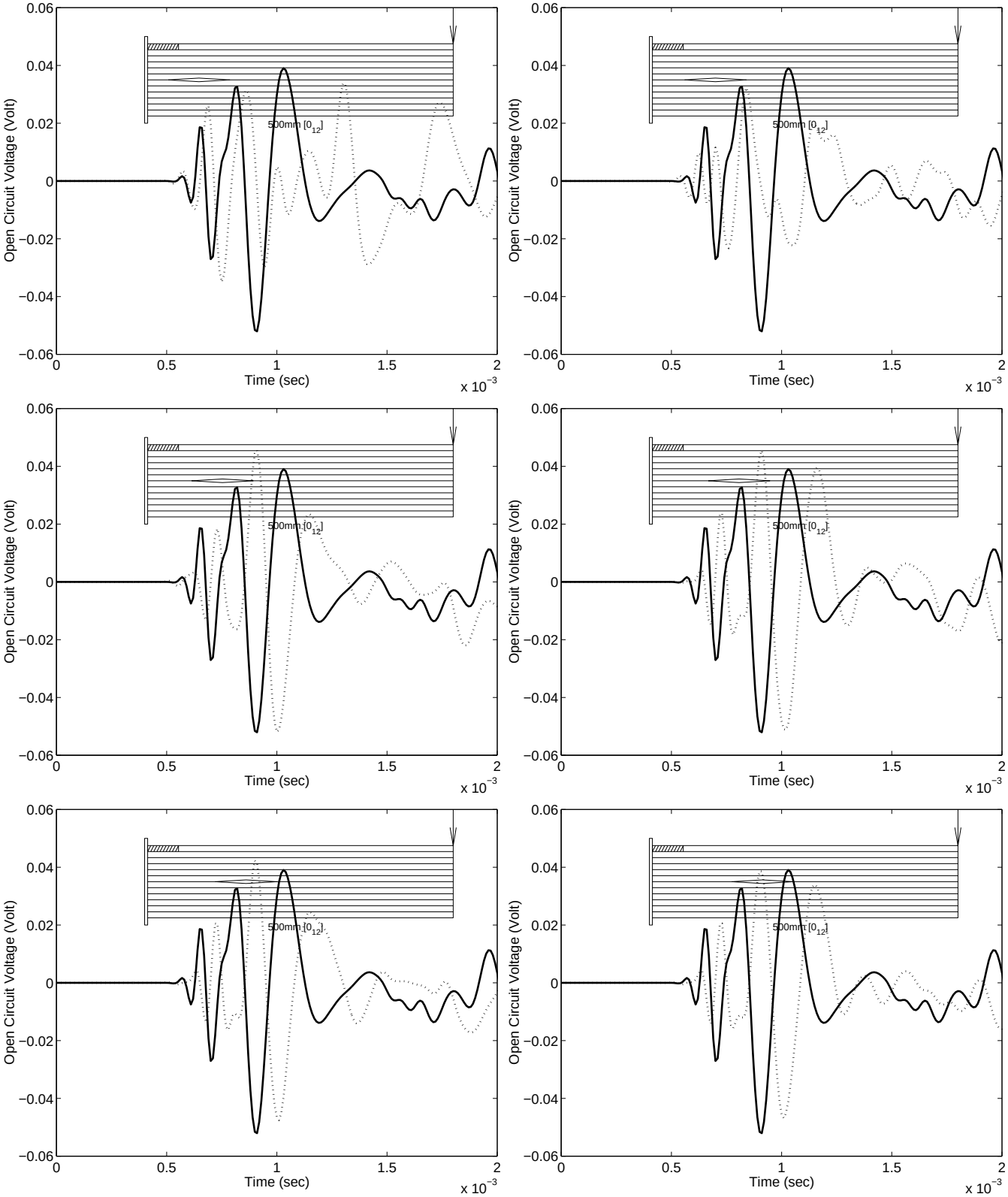

Figure 6.13: 100mm Mid Layer Delamination for Different Distance from Support.

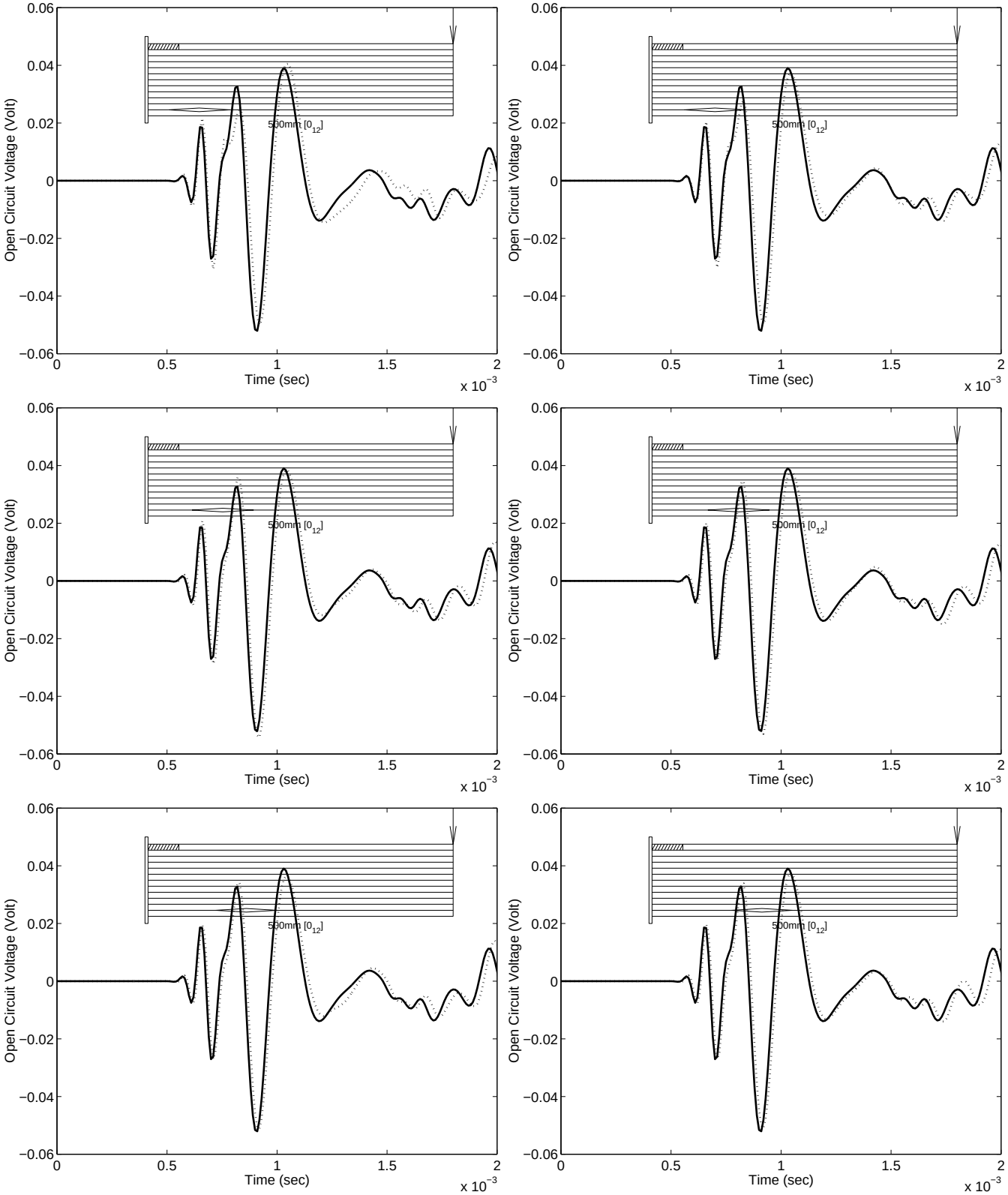

Figure 6.14: 100mm Bottom Layer Delamination for Different Distance from Support.

delamination in the sensor open circuit voltages are negligible. Hence it is very difficult to identify the delamination from sensor open circuit voltages, if delamination is with in this location.

Figure-6.15 shows the open circuit voltages for 20mm top layer delamination for different distance (40, 50, 60, 70, 80, and 90mm) from support. The effects of delaminations are negligible when the delaminations are 40 and 90mm from support. For delamination of 50 or 70mm distant from support, the response difference from healthy response is only at end part of the time window. However, for delamination of 60mm distant from support, this difference is only at beginning part of the response.

6.3.2.3 Multiple Delaminations

Figure-6.16 shows the sensor open circuit voltages for multiple delaminations increasing in sizes towards the depth of the laminate. Unlike tip response, the change of peak amplitude and peak location of sensor responses are varied monotonically from three layer delaminations to six layer delaminations, which can be used for identification of delamination easily.

6.3.3 Tip Response for Actuation

Figure-6.17 to Figure-6.22 are the vertical velocity histories of the tip of the cantilever due to 50 Hz (shown in the Figure-3.6(a)) and 5 kHz (shown in the Figure-3.6(b)) actuation current in a 50mm long actuator placed at bottom layer near support. For 50 Hz actuation current, Newmark integrations are performed for 0.1 sec with 100 steps and 1 mili-sec time steps. For 5 kHz actuation current, it is done for 1 mili-sec with 100 steps and 0.01 mili-sec time steps. Waves are propagated from actuator to tip of the cantilever in around 3 mili-secs hence tip velocity response of first 3 mili-secs are zero.

6.3.3.1 Varying Location

Figure-6.17 to Figure-6.19 gives response histories for different delamination location from the support to 200mm distance in 20 delamination steps each of 10 mm. Figure-6.17 shows the cantilever tip velocity for 100mm delamination at top layer. For 50 Hz actuation (left), effect of delamination location is negligible, where as for 5 kHz actuation (right) maximum peak tip velocity of the cantilever is when the delamination is near the support. Subsequently, it has reduced when the delamination is 30mm distant from support. Again

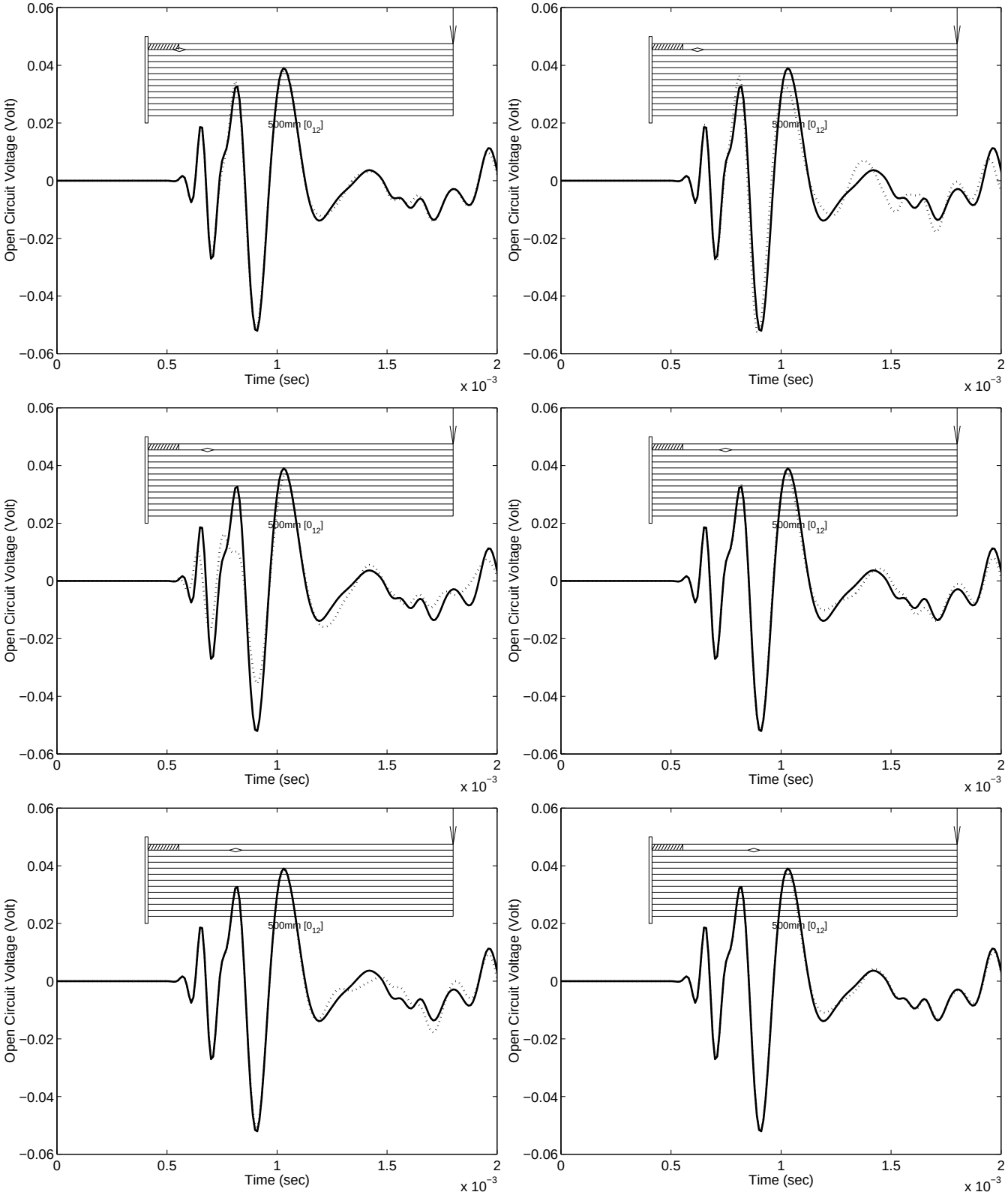

Figure 6.15: 20mm Top Layer Delamination for Different Distance from Support.

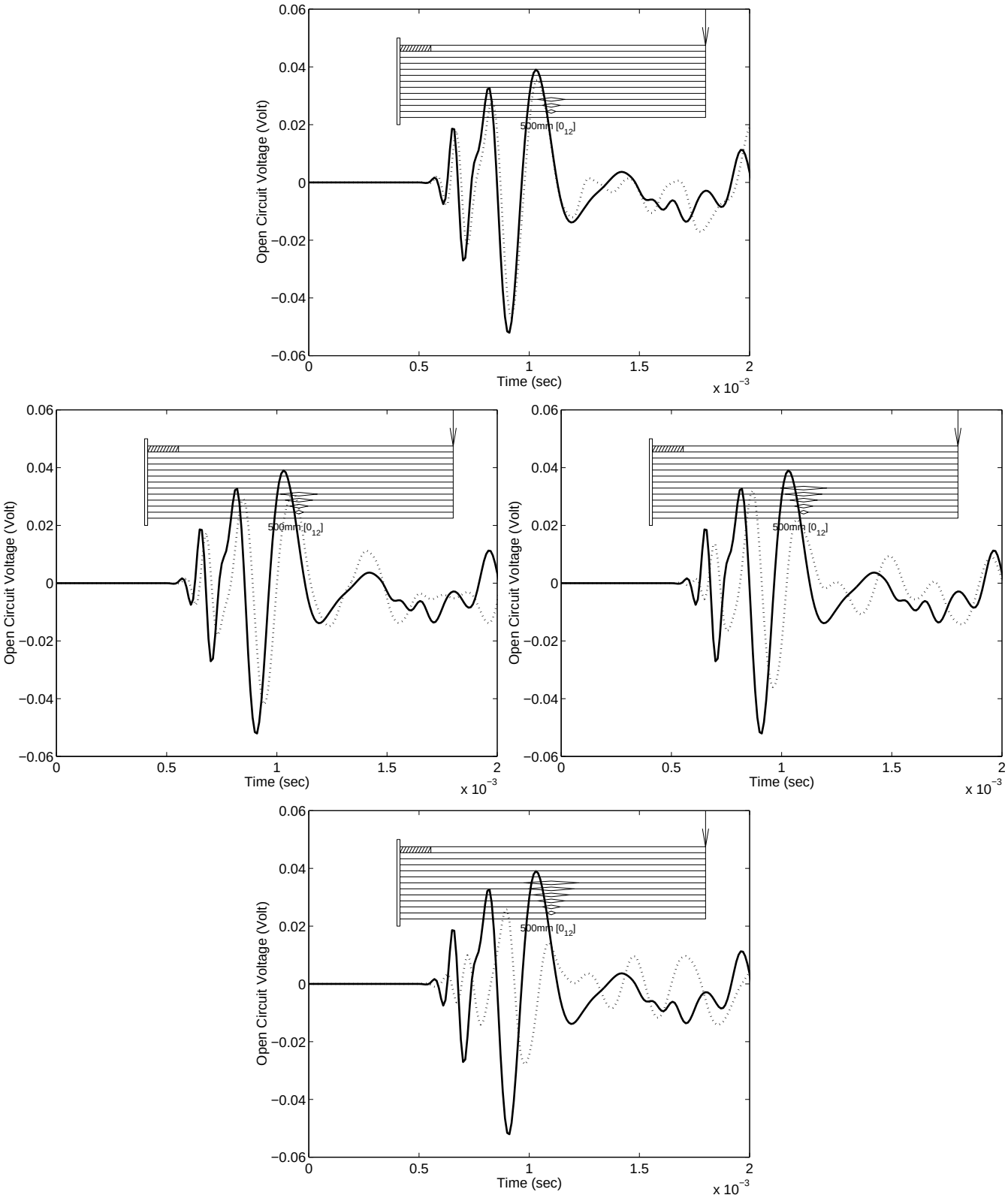

Figure 6.16: Multiple Delaminations Increasing towards the Depth

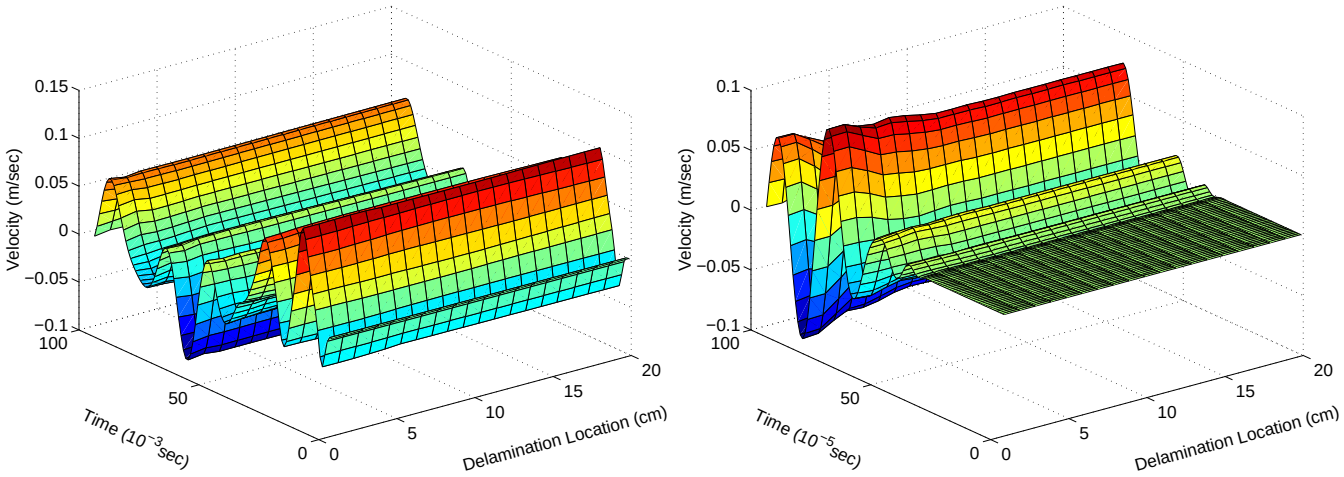

Figure 6.17: 100mm Delamination at Top layer for 50 Hz and 5kHz Actuation.

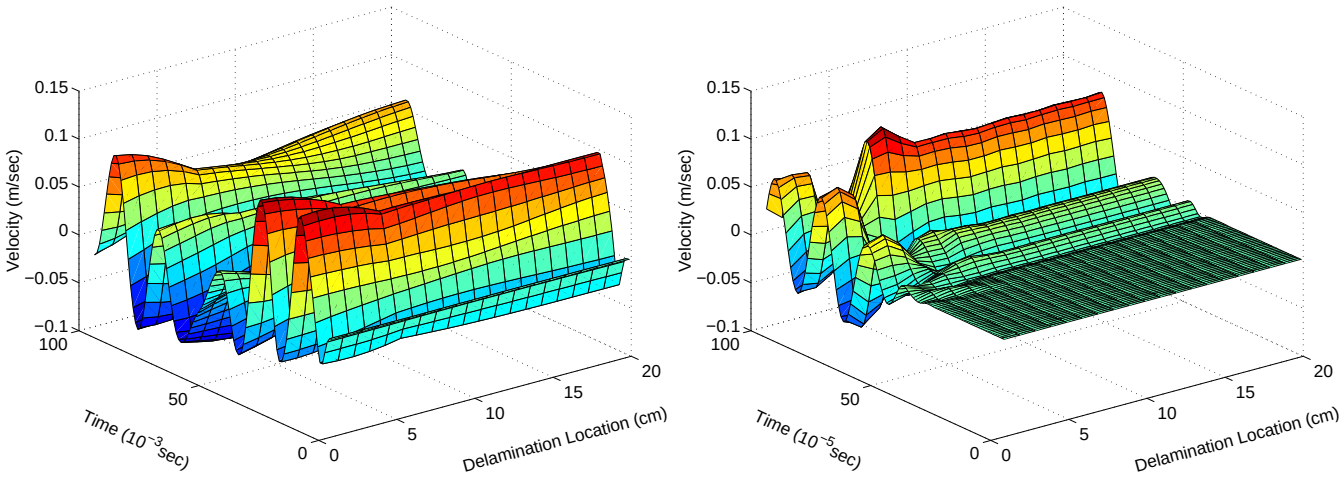

Figure 6.18: 100mm Delamination at Mid layer for 50 Hz and 5kHz Actuation.

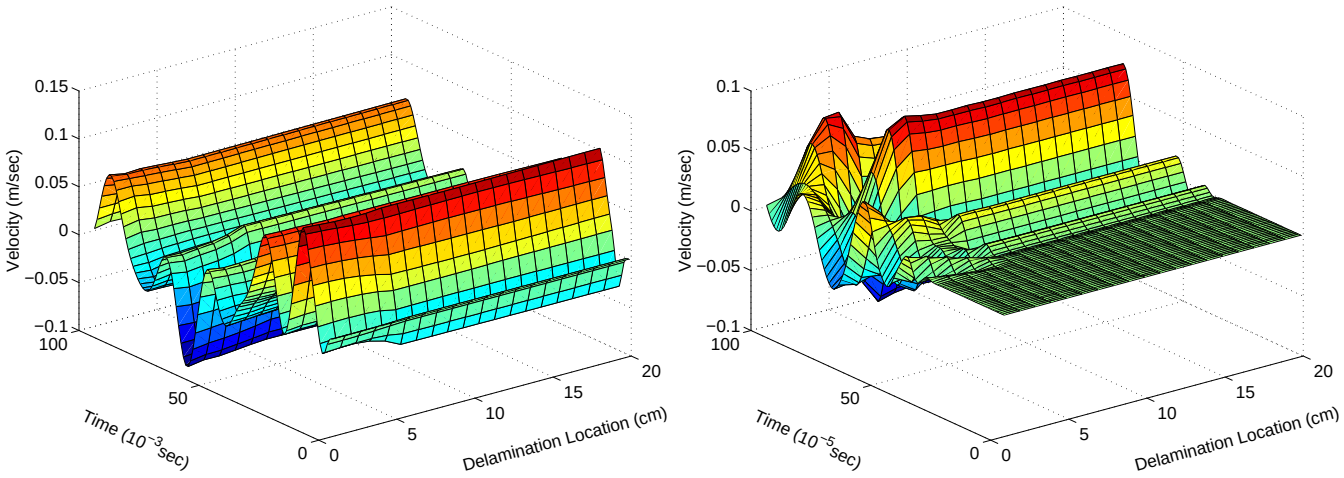

Figure 6.19: 100mm Delamination at Bottom layer for 50 Hz and 5kHz Actuation.

it goes to maximum at 50mm, where delamination starts from the end of the actuator span. After 100mm the effect of delamination location is again negligible.

Figure-6.18 shows the cantilever tip velocity for 100mm delamination at mid layer. Unlike top layer delamination, for 50 Hz actuation (left), effect of delamination location is noticeable. Maximum peak tip velocities are when the delaminations are near the support or at the 200mm apart from the support. For 5 kHz actuation (right) peak tip velocity of the cantilever is when the delamination is 50mm apart from the support and minimum just before this location. Like top layer, after 100mm, the effect of delamination location is again negligible. Early arrivals of waves are observed for delamination location from support to 50mm, which is due to increased of wave speed for reduced thickness of sub-laminate connected with actuator.

Figure-6.19 shows the cantilever tip velocity for 100mm delamination at bottom layer. Like top layer delamination, for 50 Hz actuation (left), effect of delamination location is negligible. For 5 kHz actuation (right) peak tip velocity of the cantilever is when the delamination is 50mm apart from the support and minimum is just before that. After 100mm the effect of delamination is again negligible. Like mid layer, Early arrival of stress waves are observed for delamination location from support to 50mm, which is due to farther reduction of sub-laminate thickness connected with actuator.

Hence, with 50Hz actuation frequency, delamination at mid layer and with 5kHz frequency, delamination near the actuator can be identified using cantilever tip response histories. Moreover, early arrival of stress wave in tip response can give an indication of the thickness of sub-laminate connected to the actuator for delamination.

6.3.3.2 Varying Size

In this study, size of delamination is varied to study the effect of size of delamination on tip response histories of cantilever beam. Figure-6.20 to Figure-6.22 shows response histories for different delamination sizes from 0mm to 200mm near the support in 20 steps of 10 mm.

Figure-6.20 shows the cantilever tip velocity for varying delamination lengths near support at the top layer. For 50 Hz actuation (left), effect of delamination size is negligible; where as for 5 kHz actuation (right), tip velocity is increased for longer delamination sizes.

Figure-6.21 shows the cantilever tip velocity for varying delamination lengths near support at the mid layer. Unlike the top layer, for 50 Hz actuation (left), effect of delamination size is considerable and two peaks are visible in the direction of delamination.

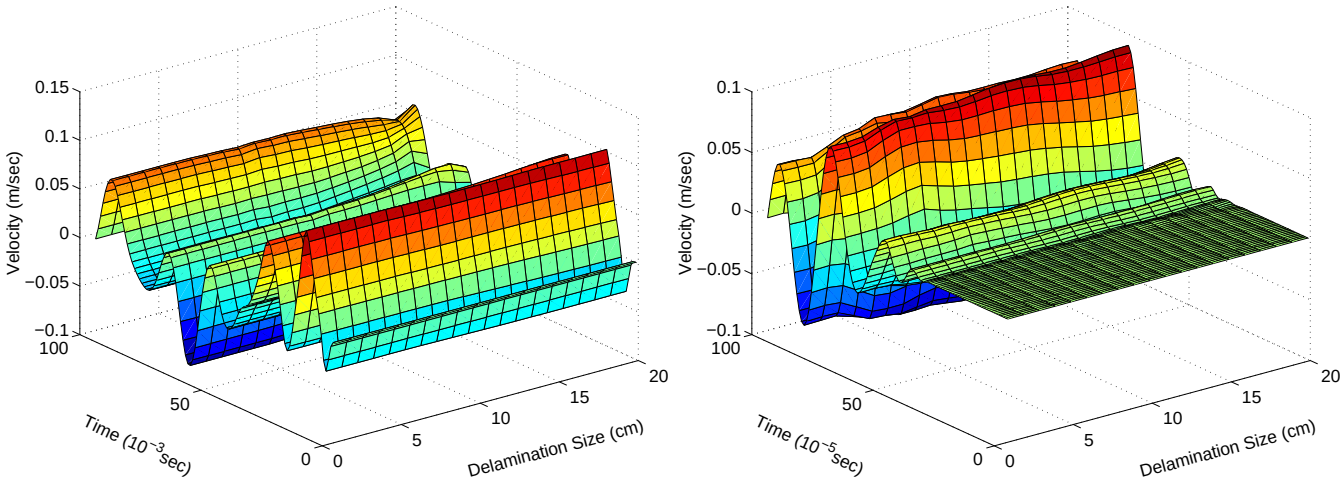

Figure 6.20: Delamination at Top layer near support for 50 Hz and 5kHz Actuation.

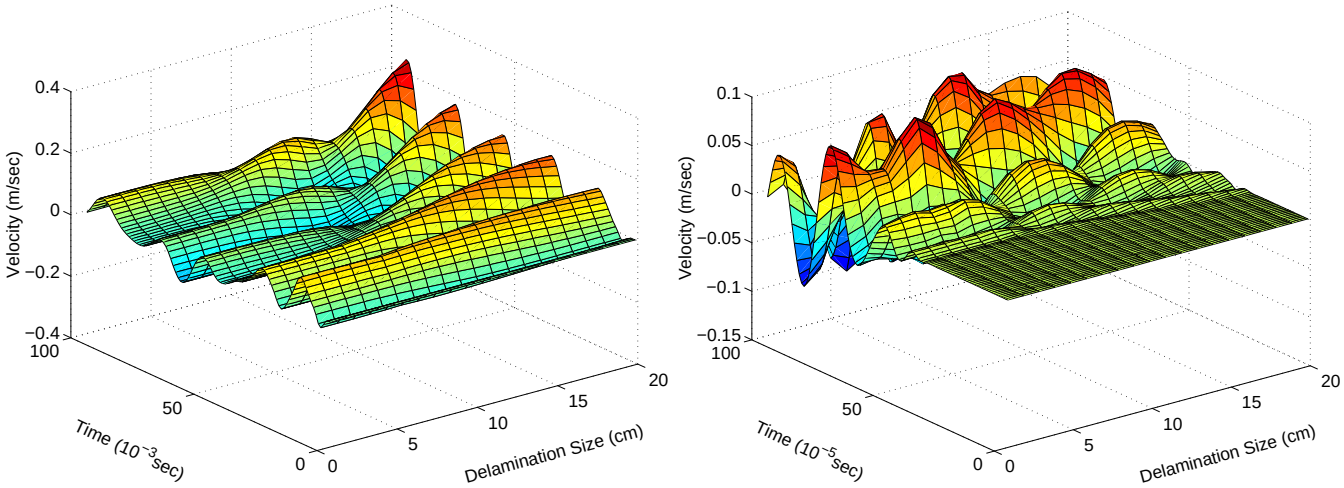

Figure 6.21: Delamination at Mid layer near support for 50 Hz and 5kHz Actuation.

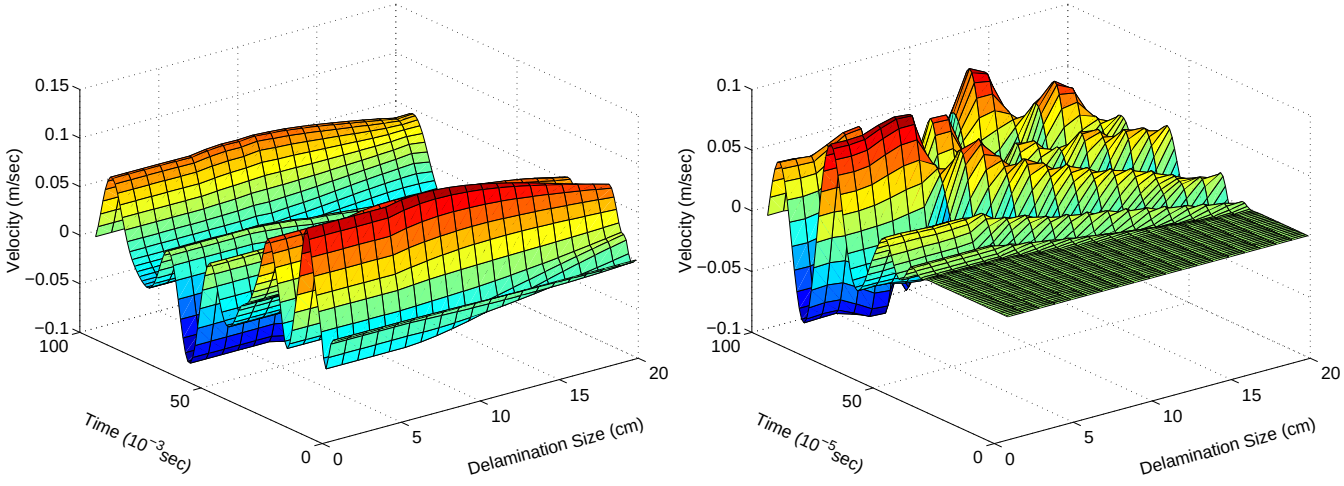

Figure 6.22: Delamination at Bottom layer near support for 50 Hz and 5kHz Actuation.

For 5 kHz actuation (right), various local peaks are seen. In addition, earlier arrivals of responses are observed due to reduction of thickness of actuator sub-laminate.

Figure-6.22 shows the cantilever tip velocity for varying delamination length near support at bottom layer. For 50 Hz actuation (left), one flat peak is seen in the velocity history plot, which indicates that for 100 mm delamination at the bottom layer near support gives maximum sensitivity in tip response for 50Hz actuation frequency. For 5 kHz actuation (right), various local peaks are seen as before. In addition, for 60mm delamination, when the delamination is just separating actuator and rest of the beam, velocity history is decreased considerably and early arrival of stress wave in response history is observed due to reduction of actuator sub-laminate thickness.

6.3.4 Sensor Response for Actuation

Figure-6.23 to Figure-6.28 are the open circuit voltages of the sensor due to 50 Hz (shown in the Figure-3.6(a)) and 5 kHz (shown in the Figure-3.6(b)) actuation current given to the actuator. 50 mm long sensor and actuator are placed at the top and bottom layer and near the support of cantilever.

6.3.4.1 Varying Location

Figure-6.23 shows the sensor open circuit voltage history for 100mm delamination at top layer with different distance from support. When the delamination separates the sensor from rest of the beam (delamination 50mm away from support), open circuit voltages reduce for 50 Hz actuation, where as it increases for 5kHz actuation. For delamination beyond sensor location, the sensor open circuit voltages predicted is negligible for both the cases.

Figure-6.24 shows the sensor open circuit voltage history for 100mm delamination at mid layer with different distance from support. When the delamination is at the middle layer, the effect of delamination location in the sensor open circuit voltages are noticeable for both 50Hz and 5kHz actuation frequency. For 50 Hz actuation, two peak maximum responses are available, one at near the support and other at 200mm apart from support. For 5 kHz actuation, a number of peaks ca be seen, which can be used in delamination identification procedure from sensor response histories.

Figure-6.25 shows the sensor open circuit voltage history for 100mm delamination at bottom layer with different distance from support. Similar to top layer, when the delamination separates the actuator from rest of the beam (delamination 50mm away from

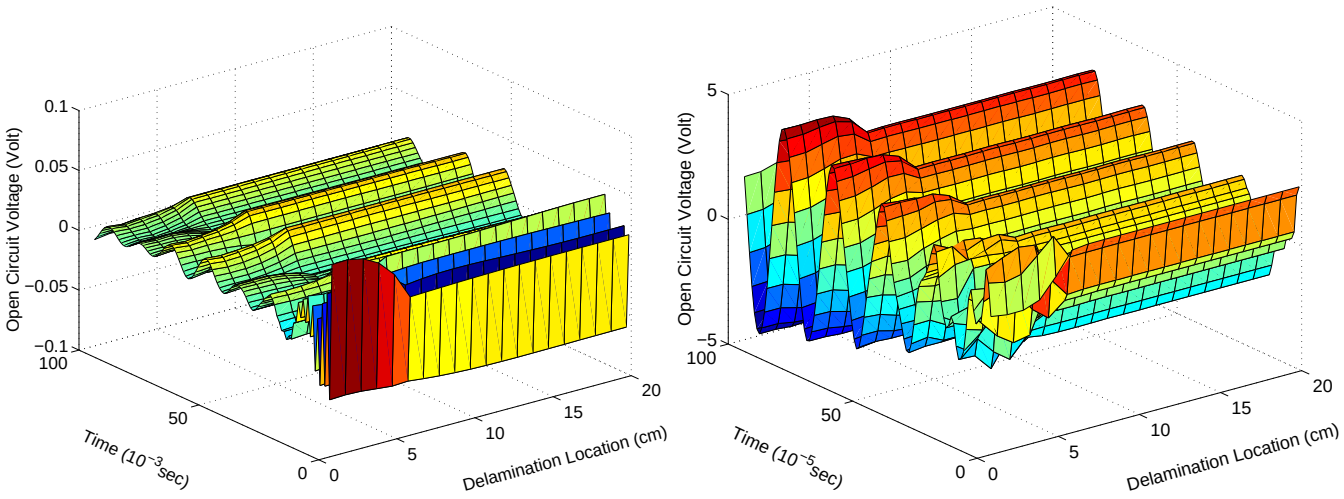

Figure 6.23: 100mm Delamination at Top layer for 50 Hz and 5kHz Actuation.

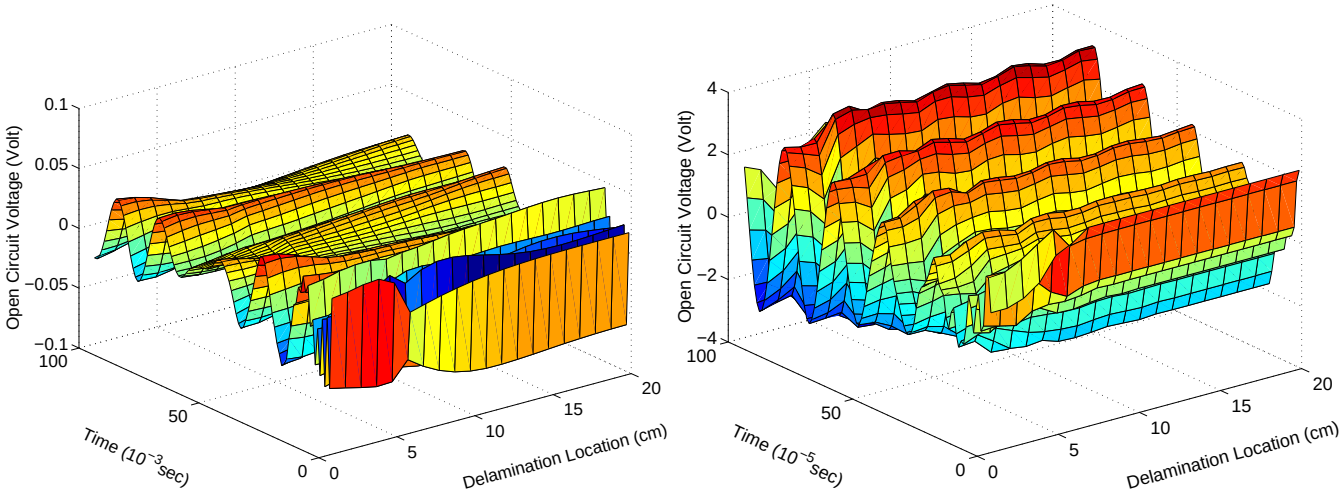

Figure 6.24: 100mm Delamination at Mid layer for 50 Hz and 5kHz Actuation.

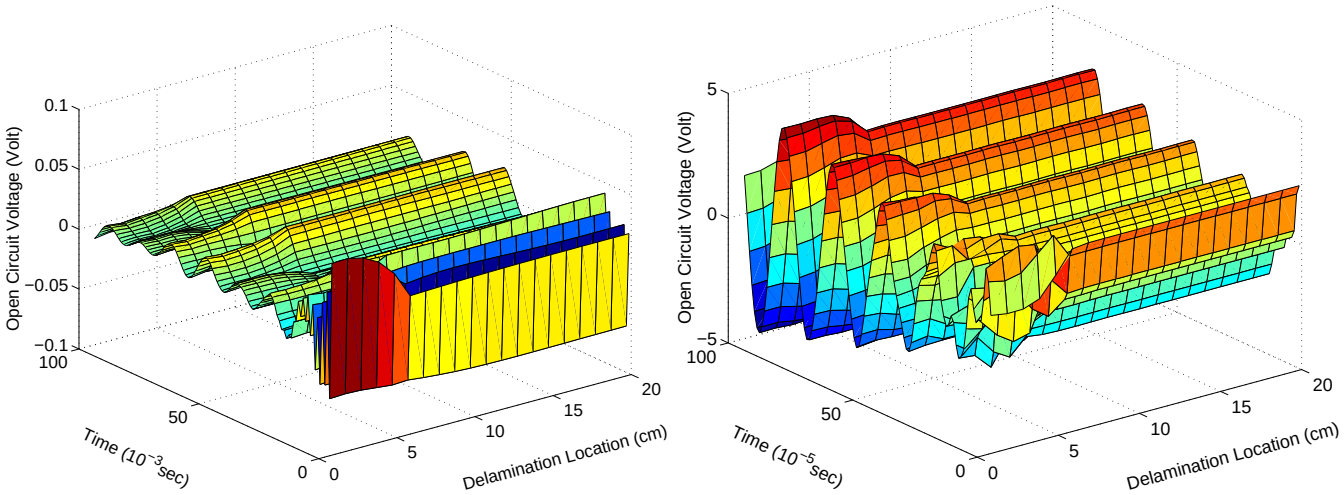

Figure 6.25: 100mm Delamination at Bottom layer from support to 200mm for 50 Hz and 5kHz Actuation.

support), open circuit voltages reduce for 50 Hz actuation, where as it increase for 5kHz actuation. Similar results are observed for top layer delamination, when delamination separates the sensor from rest of the beam. This sensor-actuator reciprocity is observed for other layers of delamination when sensor and actuator are symmetrically placed on both side of the neutral axis of the beam. This is one of the important information required for optimal placements of sensor and actuator in structural health monitoring problem. For delamination beyond actuator location, the change in sensor open circuit voltages is negligible for both the cases.

Hence, using 50Hz or 5kHz actuation, delamination near the sensor and/or actuator can be identified. Moreover, using 5kHz actuation, mid layer delamination can be identified effectively.

6.3.4.2 Varying Size and Layer

Figure-6.26 shows the sensor open circuit voltage history for different size of delamination at top layer near support. When the delamination separates the sensor from rest of the beam (more than 50mm delamination from support), larger delamination reduce the open circuit voltages for 50 Hz actuation, where as it increases for 5 kHz actuation.

Figure-6.27 shows the sensor open circuit voltage history for different size of delamination at mid layer near support. When the delamination is at the middle layer, the effect of delamination size in the sensor open circuit voltages can be used for identification. For 50 Hz actuation, two peak maximum responses are seen along the direction of delamination size, one for 100mm and other 200mm delamination. For 5 kHz actuation a number of peaks are seen as before, which can be used efficiently for identification of delamination.

Figure-6.28 shows the sensor open circuit voltage history for different size of delamination at bottom layer near support. When the delamination separates the actuator from rest of the beam, larger delamination reduce the open circuit voltages for 50 Hz actuation, where as it increases for 5 kHz actuation. Similar results are observed for top layer delamination, due to symmetric sensor-actuator reciprocity of the delamination location mentioned in earlier paragraph.

In the above discussion, it is shown that the combination of magnetostrictive sensor and actuator are sensitive to the delamination of size 50mm in composite laminate, which can be used to identify the location of delamination.

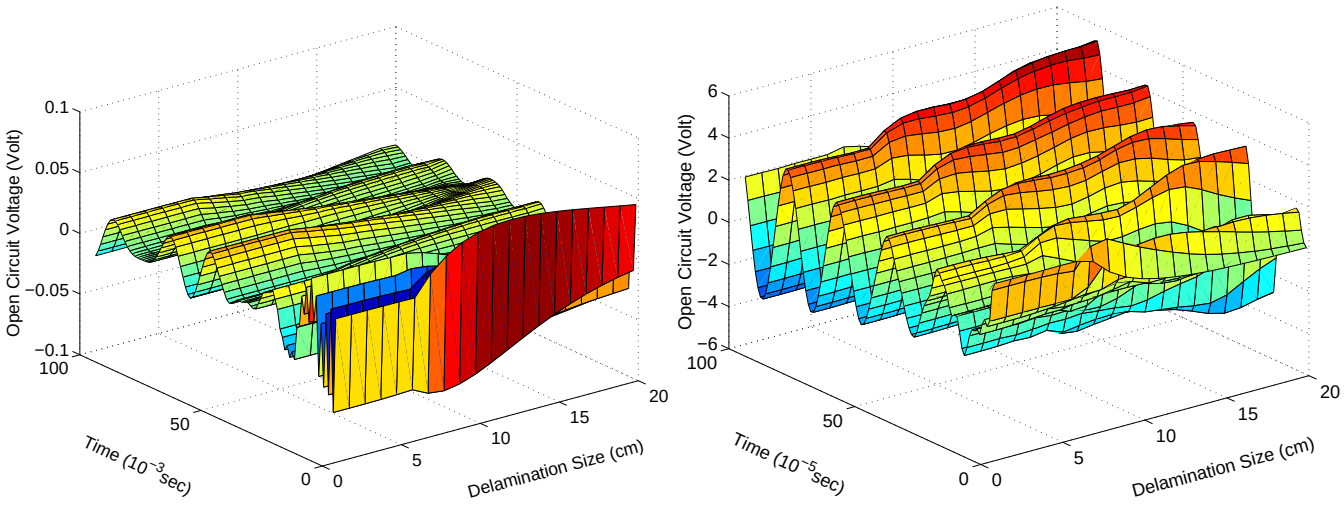

Figure 6.26: Delamination at Top layer near support for 50 Hz and 5kHz Actuation.

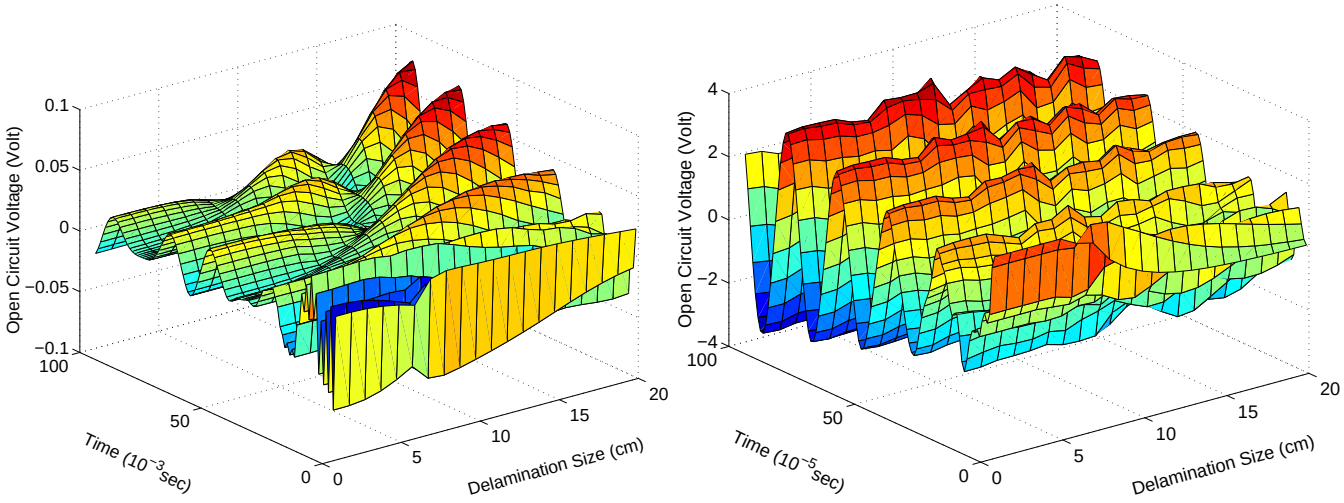

Figure 6.27: Delamination at Mid layer near support for 50 Hz and 5kHz Actuation.

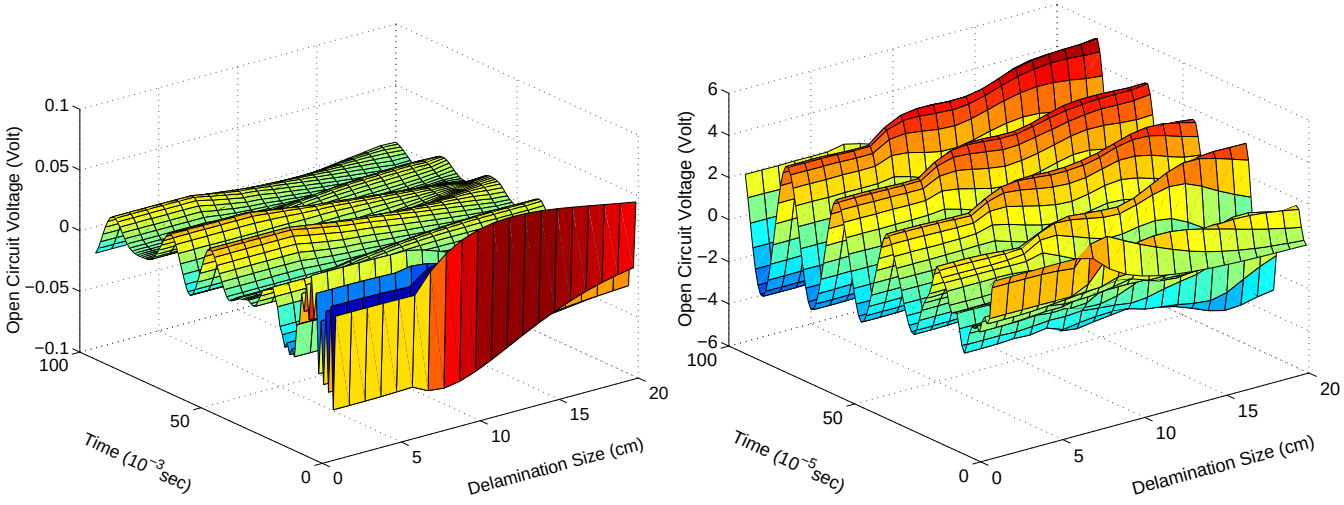

Figure 6.28: Delamination at Bottom layer near support for 50 Hz and 5kHz Actuation.

6.3.5 SHM of a Portal Frame

In this subsection, numerical simulations are performed on a portal frame to study the effect of the location of sensors on delamination sensing of structural health monitoring. Two portal frames with thick and thin members are considered to study these effects considering different beams or 2D assumptions. Figure-6.29 shows the delaminated

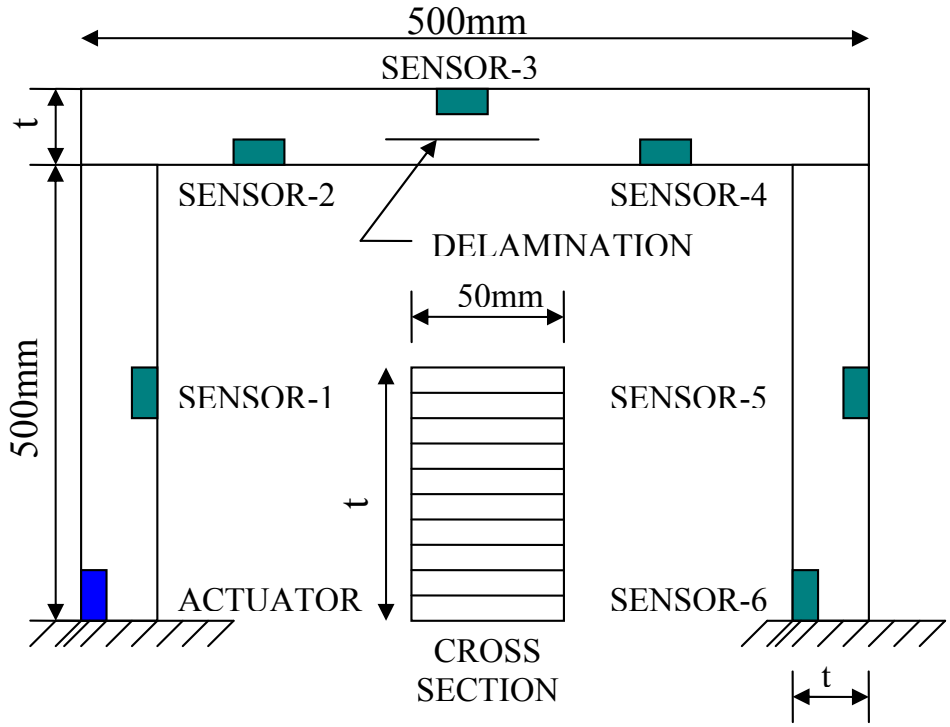

Figure 6.29: Delaminated Composite Portal Frame with Sensors and Actuator

Table 6.1: Locations of different sensors and actuator

Actuator	Left Member Outer Layer near Support
Sensor-1	Left Member Inner Layer 225mm form Support
Sensor-2	Top Member Bottom Layer 100mm from Left end
Sensor-3	Top Member Top Layer 225mm from Left end
Sensor-4	Top Member Bottom Layer 100mm from Right end
Sensor-5	Right Member Outer Layer 225mm from Support
Sensor-6	Right Member Inner Layer near Support

composite portal frame with six sensors and one actuator. Lengths of the members of the portal frames are of 500mm each. Thicknesses (t) for thin and thick portal members are considered as 10mm and 50mm with 10 layers of unidirectional composite, respectively.

Fixed location of the delamination is considered in this study, which is at the middle and mid-layer of the horizontal frame member. Size of the magnetostrictive actuator and sensors are considered as 50mmX50mm. Locations of the sensors and actuator are given in Table-6.1 and shown in Figure-6.29. Material properties are taken as per earlier simulation of this section. Number of coil turn in sensors and actuator are 2000 turn/m (100turn).

Figure-6.30 to Figure-6.35 are the open circuit voltages of the sensors due to 5 kHz (shown in the Figure-3.6(b)) actuation current in the 50mm long actuator placed near support. Newmark integrations are performed for 1 mili-sec with 100 steps and 10 μ-sec time step each.

6.3.5.1 Thin Portal Frame

Figure-6.30 to Figure-6.33 show the open circuit voltages in different sensors for thin portal frame with or without delamination. Waves are propagated from actuator to the other side of the frame in around 0.3 mili-sec, hence sensor responses are zero as long as the stress waves are not reaching to the respective sensor locations. Figure-6.30 shows the sensor responses of a healthy portal frame considering classical (EB), FSDT beam and 2D assumptions. Response in SENSOR-1 is maximum (0.15 volt) among other sensors, as it is near the actuator. Similarly, minimum (0.05 volt) sensor response is in the SENSOR-5 and SENSOR-6, which are placed in the other leg of the frame. Responses from beam assumption are almost similar to 2D assumption for SENSOR-2, SENSOR-3, SENSOR-4 and SENSOR-6. Deviations of the responses for beam assumptions are considerable for SENSOR-1 and SENSOR-5. Using EB and FSDT beam assumptions, SENSOR-1 shows 80 and 30 mili-volt less amplitude than 2D analysis, where as SENSOR-5 shows 15 and 5 mili-volt more amplitude than 2D analysis, respectively.

Figure-6.31 shows the sensor responses for different delamination size (0mm, 20mm, 50mm and 100mm) considering EB beam assumptions. Response in SENSOR-1 is similar to healthy beam up to 0.3 mili-sec, which is the time taken to return back the reflected wave from the delamination tip. 100mm delamination shows 50 mili-volt voltage differences, which is less than the required sensitivity for this sensor; hence 100mm delamination is not detectable by SENSOR-1. Similar to SENSOR-1, SENSOR-2 is also located before the delamination and the stress waves are reflected back to the SENSOR-2 at 0.2 mili-sec. Response difference for both 50mm and 100mm delaminations are above 50 mili-volts. Hence, SENSOR-2 can be used to detect delamination up to 50mm size. SENSOR-3 is

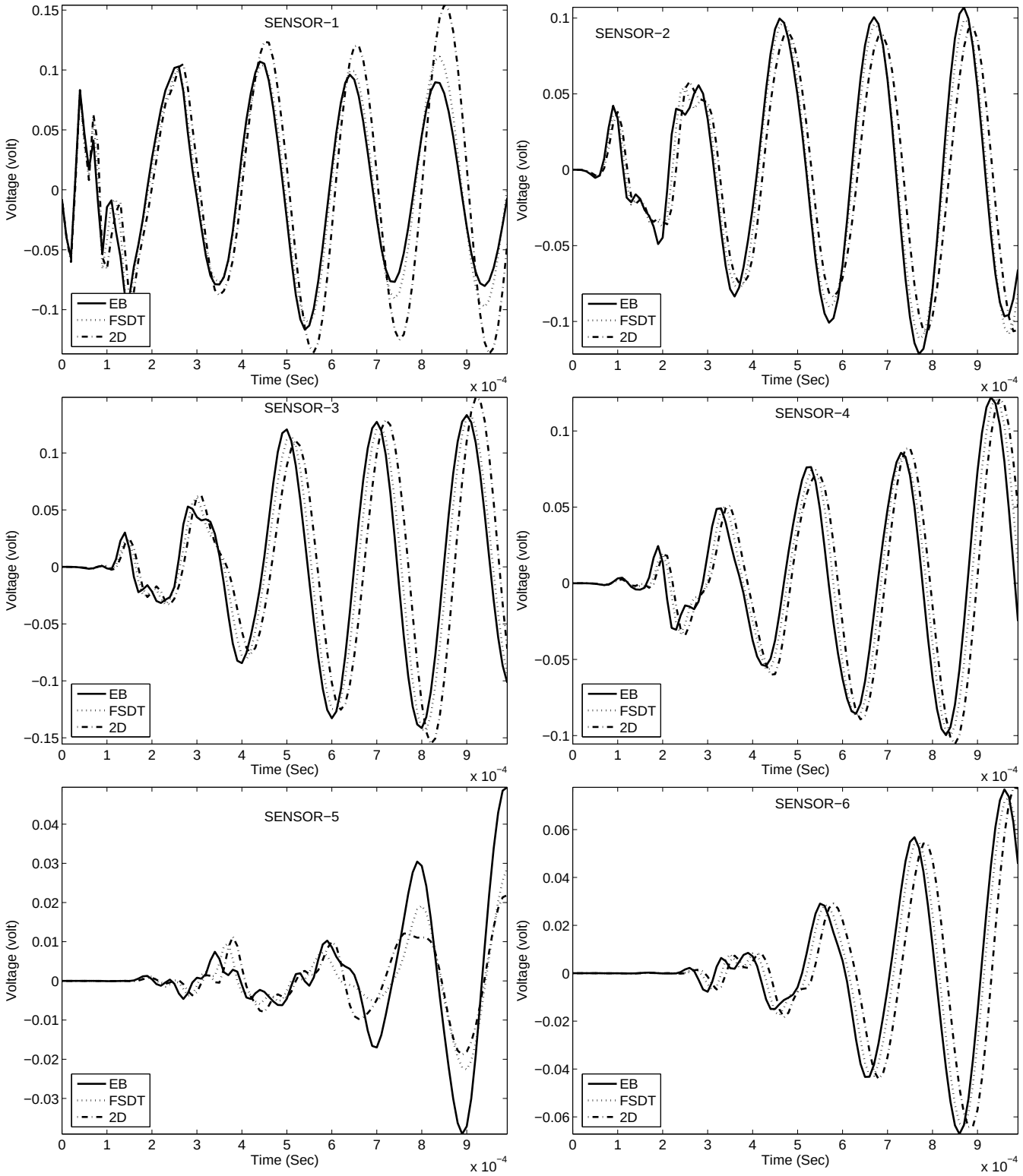

Figure 6.30: Sensor Responses for Different Beam Assumptions.

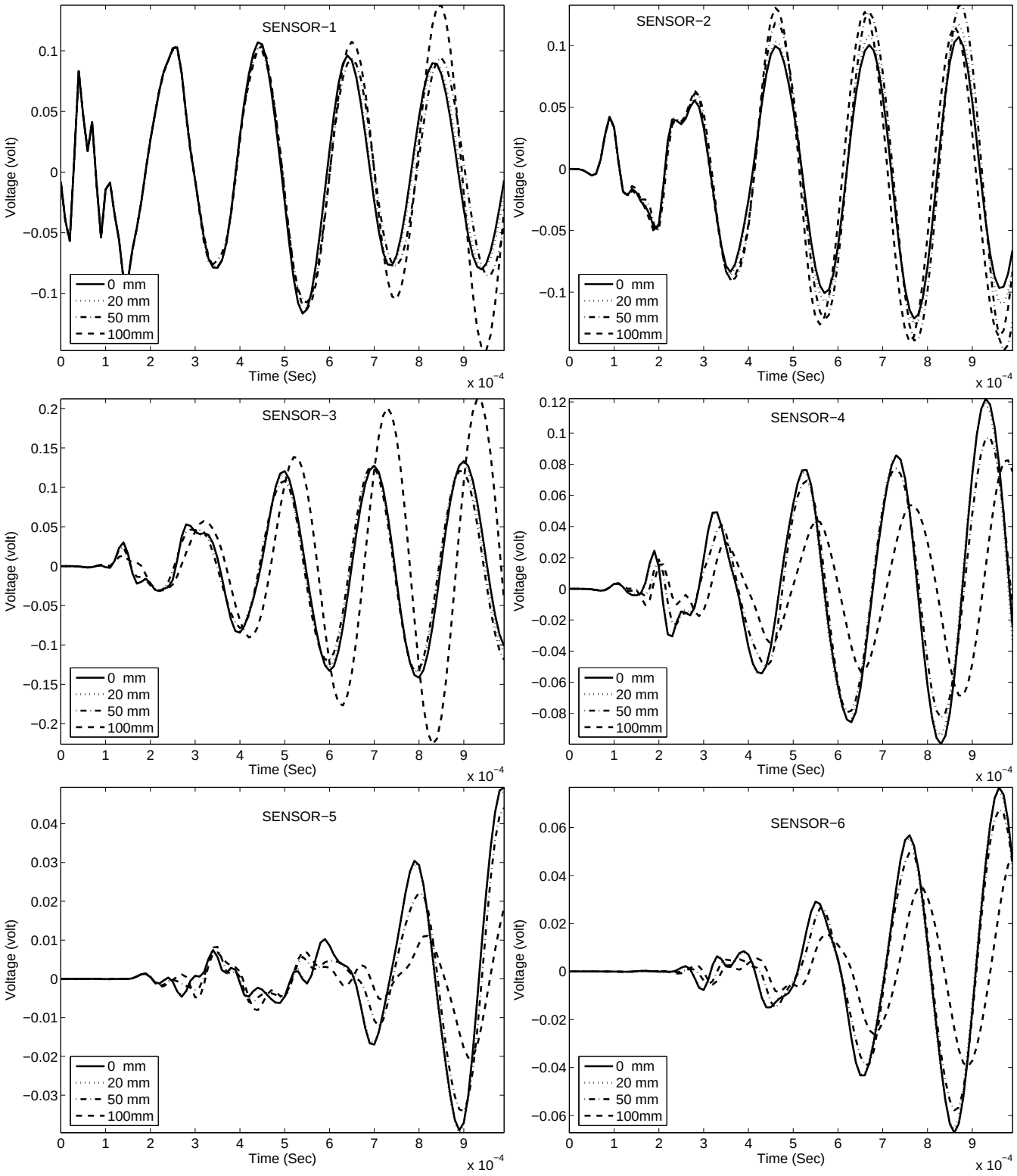

Figure 6.31: Sensor Responses for Different Locations of Sensors with EB Assumption.

located just ahead of the delamination. Hence, the response deviation started when the wave reached to the sensor. Phase shift is also observed in the response for 100mm delamination. Hence, this sensor can detect 100mm delamination efficiently. SENSOR-4, SENSOR-5 and SENSOR-6 are located in the other side of the delamination from actuator. Hence, considerable amount of phase shift are observed for these responses. The response differences between healthy and delaminated frames can be used to detect 50 to 100mm delamination by these sensors.

Figure-6.32 shows the sensor responses for delaminated frame considering FSDT beam assumptions. Similar to EB formulation, SENSOR-1 shows 50 mili-volt differences for 100mm delamination. Hence, delamination sensitivity of SENSOR-1 can be considered as 100mm. SENSOR-3, which is located just above the delamination, can detect 100mm delamination efficiently. Similar to EB assumption, SENSOR-2, SENSOR-4, SENSOR-5 and SENSOR-6 can detect 50 to 100mm delamination.

Figure-6.33 shows the sensor responses for delaminated frame considering 2D model. SENSOR-1 to SENSOR-3 doesn't have any phase shift in the delaminated response, where as SENSOR-4 to SENSOR-6 show phase differences. If the sensor and actuator are in either side of the delamination, this phase shift phenomena are observed. This can be used for identification of the location of delamination using responses of different sensor-actuator pairs. For SENSOR-3, both beam 1D models show considerable phase shift, which is absent in 2D model.

6.3.5.2 Thick Portal Frame

Figure-6.34 and Figure-6.35 shows the open circuit voltages in different sensors for thick, healthy and delaminated portal frames. Waves are propagated from actuator to other leg of the frame in around 0.12 mili-sec, hence sensor responses are zero as long as the stress waves are not reaching to the respective sensor locations. Figure-6.34 shows the sensor responses of healthy portal frame considering classical, FSDT beam and 2D assumptions for their relative usefulness in SHM. Response histories in SENSOR-1 and SENSOR-2 from EB assumption show more than double response than 2D assumption. Hence, for a thick portal, EB assumption is not suitable. Even, most of the sensors responses show considerable deviation between the FSDT and 2D models. Hence, beam assumption for thick portal frame is not suitable for SHM application and only 2D analysis is performed for the response of the delaminated beam.

Figure-6.35 shows the sensor responses for delaminated portal frame considering

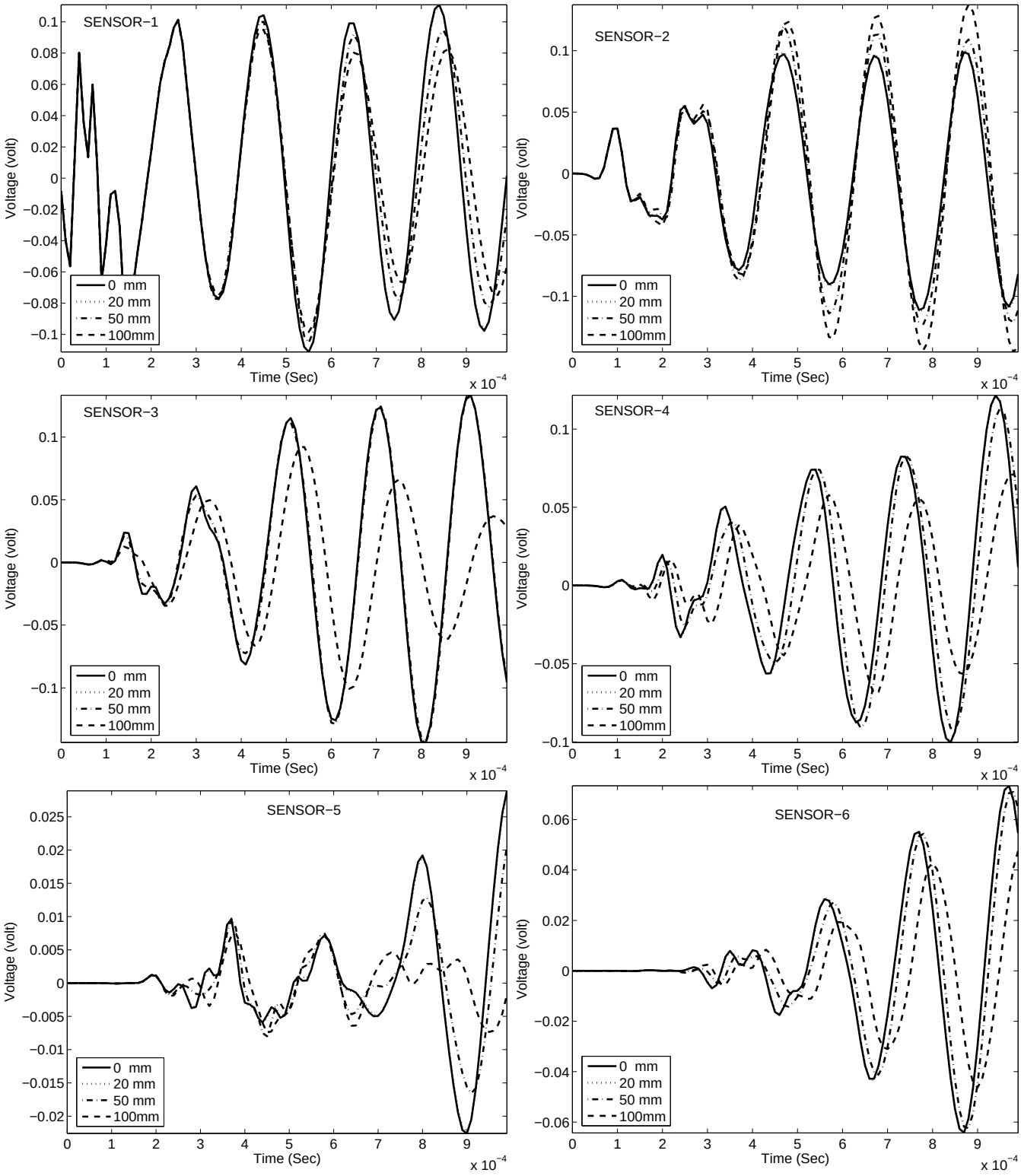

Figure 6.32: Sensor Responses for Different Locations of Sensors with FSDT Assumption.

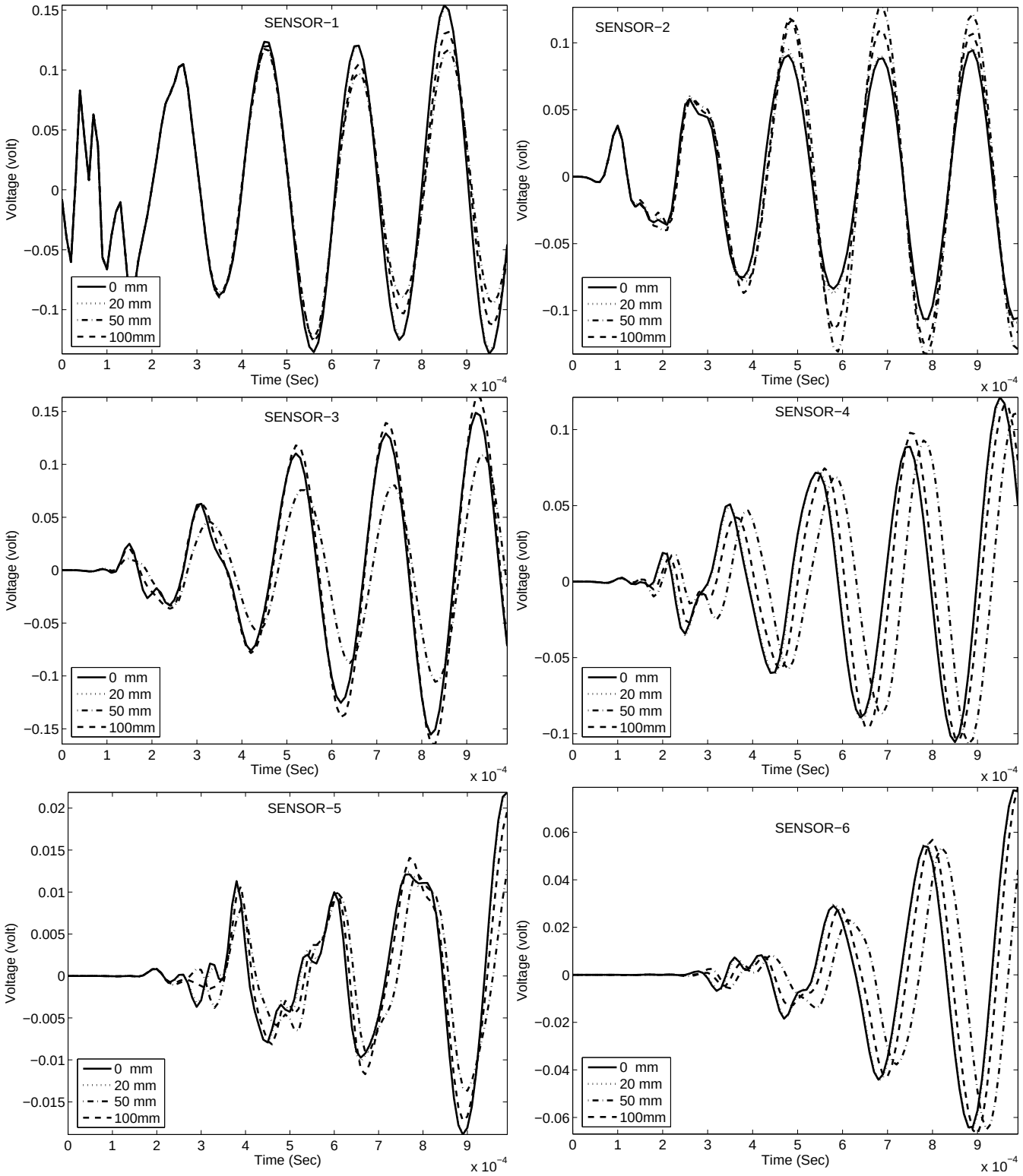

Figure 6.33: Sensor Responses for Different Locations of Sensors with 2D Model.

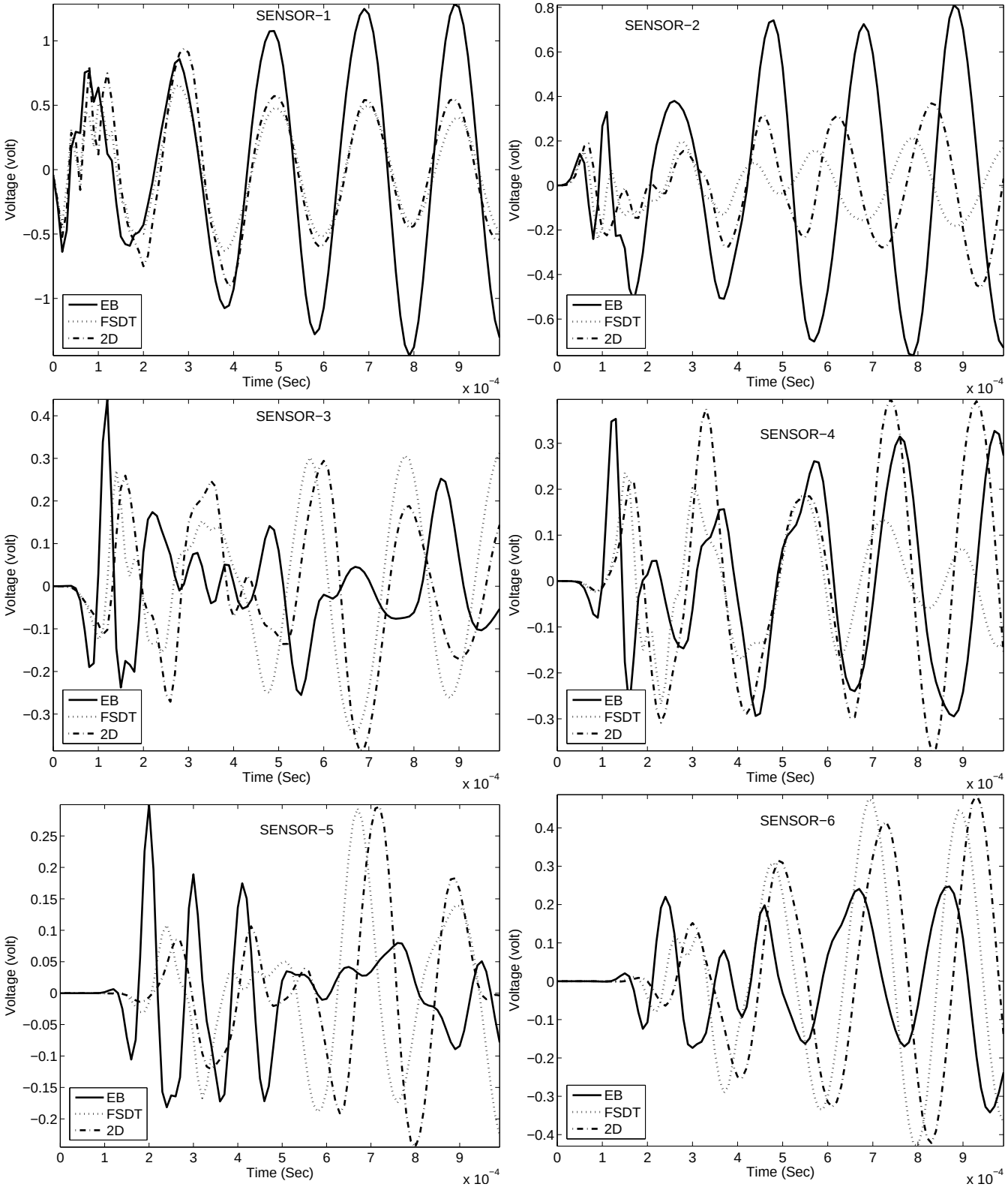

Figure 6.34: Sensor Responses for Different Beam Assumptions.

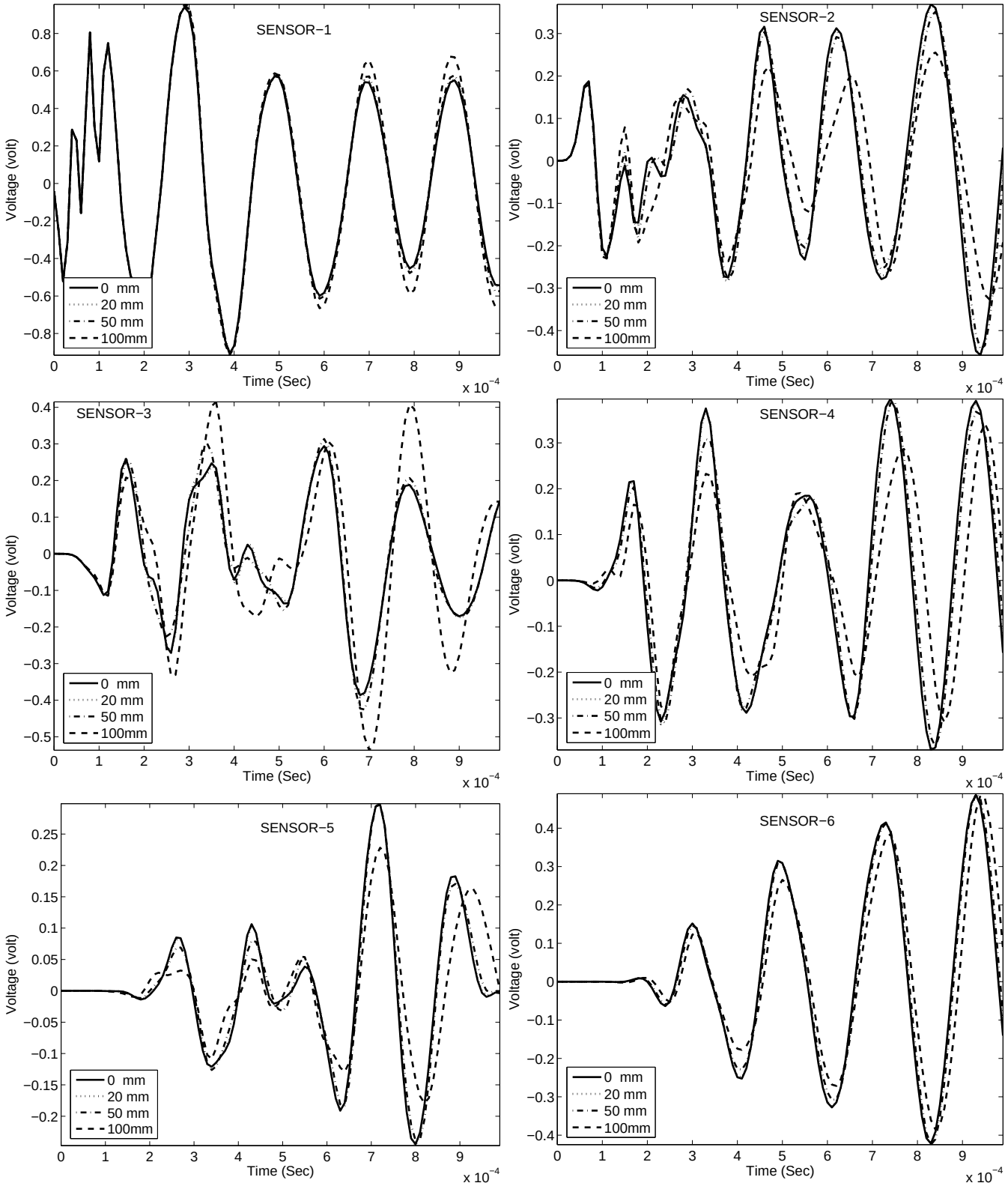

Figure 6.35: Sensor Responses for Different Locations of Sensors with 2D Model.

2D assumptions. SENSOR-1, SENSOR-2 and SENSOR-3 are located in same side of the delamination from the actuator. Hence, the responses of these sensors are increased due to the presence of delamination. SENSOR-1 and SENSOR-2 show more than 100 mili-volt differences between healthy and 100mm delaminated frames. Hence, the sensitivity of these sensors is 100mm. As SENSOR-3 is located just above the delamination, 100mm delamination shows more than 200 mili-volt sensitivity and 50mm delamination shows more than 50 mili-volt sensitivity, which can be used for detection of 50mm delamination. SENSOR-4, SENSOR-5 and SENSOR-6 are located in other side of the delamination from actuator. Hence, phase shifts of the responses are observed. In addition, the responses of these sensors are reduced due to the presence of delamination. Both decrease of the response and phase shift can be used for detection of the delamination using these sensors.

In summary, sensor located near the delamination gives better performance; hence more number of sensors is required for structural health monitoring, which can reduce the distance between delamination and sensor. When the sensor and actuator are either side of the delamination, phase shift of the sensor response are observed. Similarly, amplitude of sensor responses are reduced when sensor and actuator are either side of the delamination and increased when they are in the same side of the delamination. This can be used to identify the location of the delamination. As the differences of sensor responses for different beam assumptions are less compared to the sensitivity of the delamination, modelling of thin portal frame for structural health monitoring using beam theory is suitable. However, for thick portal frame, 2D assumption is essential for calculation of sensor responses.

6.4 Summary

Study in this chapter is mainly intended to bring out the effect of delamination on composite laminates using FE formulation. Tip response and sensor open circuit voltages are studied due to tip impact or applied current in actuator coil. Both actuation and sensing in magnetostrictive patches have been done using magnetic coil arrangement. The study demonstrates the use of vibration response in obtaining the health information of the structure with built-in magnetostrictive sensor/actuator. The effects of sensor responses for different locations of the sensors are studied for a portal frame using different beam and 2D assumptions. For SHM, portal frame with thin members can be modelled with beam assumptions. However, for thick member, frame should be modelled with 2D plane

strain/stress assumption as the errors due to these beam assumptions in sensor responses are comparable to the sensitivity of these responses for moderate delamination. If the location of delamination is in between the sensor and actuator, amplitude of the sensor response are reduced with phase shift. On the other hand, if the sensor is between actuator and delamination, amplitude of the sensor response increased without any phase shift. This technique can be used as forward solution for detection of delamination. Creating one database for different size of delamination and location, location and size of the delamination can be identified. Inverse solution for this problem can be done using any conventional or soft search technique, and this is discussed in Chapter-7.